universität wien

MASTERARBEIT / MASTER'S THESIS

Titel der Masterarbeit / Title of the Master's Thesis

Cdk1 and its role in macrophage proliferation

verfasst von / submitted by

Stefanie Horer, BSc

angestrebter akademischer Grad / in partial fulfilment of the requirements for the degree of

Master of Science (MSc)

Wien, 2019 / Vienna 2019

Studienkennzahl lt. Studienblatt / degree programme code as it appears on the student record sheet:	UA 066 830
Studienrichtung lt. Studienblatt / degree programme as it appears on the student record sheet:	Masterstudium Molekulare Mikrobiologie, Mikrobielle Ökologie und Immunbiologie
Betreut von / Supervisor:	Assoc. Prof. Dr. Thomas Weichhart

Contents

List of Tables

List of Figures

Acknowledgments

First, I want to thank Thomas Weichhart for his support and motivation and, of course, the opportunity to work in his lab on this exciting, but sometimes really difficult project. Specials thanks also go to Nyamdelger Sukkbhataar, who taught me everything I needed to know about IHC, and Stephanie Fritsch, who showed be nearly everything, from cell culture, WB, RNA Isolation, who besides was my companion in misfortune (but at the end, we kind of figured it out). I am also very grateful to the whole lab, and the institute for their help and support. Thanks to my family, who made my entire studies possible, always love and support me, and thanks to Jonathan, who was always there for me and my complains and sorrows and who had to go through a lot of mouse stories (Sorry for that!). Thanks to everyone who helped me – you made this year really great!

1 Introduction

1.1 Macrophages

In 1884 Elie Metchnikoff was the first one to identify macrophages in the small aquatic crustacean Daphnia. Metchnikoff described them as amoeboid-like blood cells attacking and ingesting pathogens. Thus he named them Phagocytes [1].
In 1968 van Furth and Cohn proposed the Mononuclear Phagocyte System (MPS), where they separated two groups: circulating monocytes and tissue macrophages. With *in vitro* labeling experiments they showed a flow from bone marrow progenitor cells (promonocytes) to differentiated cells entering the circulation (monocytes), which migrate from the peripheral blood into the tissue, where they develop into macrophages. However, they only examined monocytes and peritoneal macrophages. Further, the irradiation studies used by van Furth and Cohn did not show tissue macrophages at steady state, but after injury [2]. Although this model by van Furth and Cohn had deficiencies, it remained the prevailing hypothesis [3].
Lately, a series of fate mapping studies provided evidence for embryonic precursors of some tissue macrophages, such as microglia and Langerhans cells, and little contribution of circulating monocytes due to local self-renewal [4, 5]. Today the MPS comprises macrophages, monocytes and dendritic cells. They play a central role in the initiation of innate and adaptive immunity, maintenance of tissue homeostasis and its recovery after injury. In higher organisms macrophages are found in every tissue. During an infection monocytes migrate from blood to the inflammation site and differentiate into monocyte-derived macrophages, where they complement tissue resident macrophages [6]. However, under certain situations expansion of macrophages at the site of infection can rely exclusively on the proliferation of resident macrophages [7].

1.2 Development

In vertebrates, myeloid cells arise from two hematopoietic waves: the primitive and definitive hematopoiesis [8].
Initially, hematopoiesis in the embryo is limited to blood islands in an extra-embryonic tissue, the yolk sac (YS). Macrophages and primitive nucleated erythrocytes are produced in this tissue. The mono- or bi-potent progenitors infiltrate the embryo after the establishment of circulation at around embryonic day 8.5 (E8.5) [8, 9]. Some of those seeded tissues, as for instance the brain, remain largely independent of adult hematopoiesis and the resident macrophage population seems to maintain themselves at steady state without any contribution of monocytes [4].
Definitive multi-lineage hematopoiesis depends on hematopoietic stem cells (HSCs), which are specified before E9.5 [8, 10]. Early definitive hematopoiesis takes place at the aorto-gonado mesonephros region (AGM) and is dependant on hematopoietic stem cells (HSCs). After E10.5 HSCs migrate and colonise the fetal liver (FL), an intermediate site before the bone marrow (BM) replaces it as the main hematopoietic organ in the perinatal period [11].
Macrophages can derive from both, the YS and definitive hematopoiesis via monocyte intermediates from the FL. However, primitive and definitive hematopoiesis overlap for a short period, thus the assignment of macrophages to their origin is difficult, as HSCs and primitive progenitors co-exist [12].
Through the development of new technologies like lineage tracing studies with pulse labeling and transcriptional profiling it is now easier to differentiate between primitive progenitors and HSCs [13].

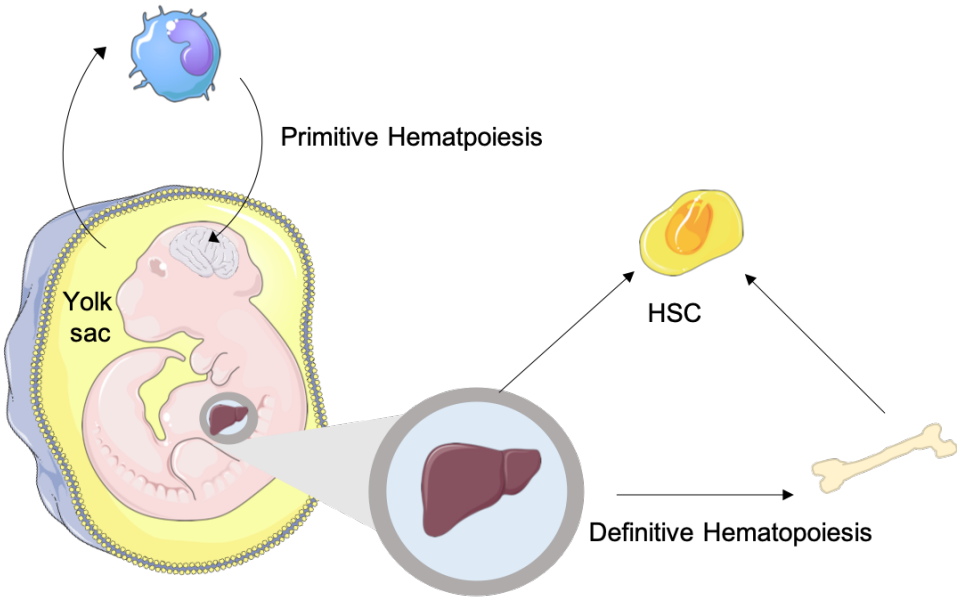

Figure 1: **Macrophage development in mice.** For further details see text.

1.3 Macrophages and proliferation (self-renewal)

As already mentioned above, some tissue macrophages are able to sustain themselves independent from monocytes. Local proliferation is the main mechanism to maintain homeostasis in steady-state conditions and to recover the macrophage pool after a challenge [6].
The ability to maintain tissue in the long-term with little input from HSCs was shown for microglia and Langerhans cells [4, 5]. Those macrophage populations derive from embryonic progenitors, which enter the tissue and expand through massive proliferative. In the adult mouse, macrophage pools, for instance in the brain or the skin, are maintained by low levels of proliferation without any input from bone marrow progenitors. The limited access to monocytic influx in the brain is due to separation from the circulation by the blood-brain-barrier in the brain or the basal lamina in the skin [4,5,14]. However, the loss of self-renewal potential of some resident macrophage populations with age might lead to an increase of monocytic contribution, especially after an infection [15].
But do all mature macrophages within a population have the same proliferative capacity or do they contain a distinct progenitor? In the latter, a specialized progenitor divides asymmetrically and gives rise to a daughter cell, which undergoes terminal maturation [16,17]. This scenario involves differentiation and change in cell identity. In the first case, any fully differentiated macrophage initiates cell division and produces equally mature macrophages, which would be a true self-renewal capacity [5].

1.3.1 Mechanism

Cytokines play an important role in macrophage proliferation. CSF1 receptor (CSF1R) ligands, CSF1 and IL-34, CSF2 and IL-4 are central regulators of proliferation. CSF2, for instance, is essential for the maintenance of the alveolar macrophage pool [18]. It also mediates restoration after irradiation [5].
Interestingly, in addition to the ability of IL-4 to drive macrophage polarization towards an alternative state [19, 20], systemic administration to mice induced proliferation in multiple tissues via the activation of the PI3K/Akt signalling cascade [21–23].
CSF1 plays a critical role in macrophage development, morphology, function and survival. Thus, it was extensively studied. Studies of the peritoneal cavity ,where CSF1 was administered, showed stimulated macrophage proliferation [24]. $CSF1^{-/-}$ mice appeared to have reduced numbers of macrophages [25]. However, microglia and Langerhans cells are unaffected by the absence of CSF1 [4,26], due to the presence of an alternative ligand for the CSF1R, IL-34 [27, 28]. This cytokine is produced by neurons and keratinocytes, which suggests an important role for the maintenance and establishment of microglial and Langerhans cell pools [29]. IL-34 and CSF1 bind to different regions of the CSF1R, but share no sequence homology [30]. Binding of one of those ligands to the CSF1R mediates activation of Ras and Erk signaling, which leads to the activation of Ets1 and Ets2. These transcription factors, in turn, activate D-type cyclins (a cell cycle regulator) and the transcription factors c-Myc and c-Myb, coordinating proliferation at the transcriptional level [31–33]. The latter is a critical factor during monocytic differentiation and its lack leads to an absence of definitive hematopoiesis [34–36]. However, macrophages evolving from the yolk sac remain completely unaffected by the presence or absence of c-Myb and

develop independently from it [14]. MafB and cMaf bind to c-Myb, mediate cell cycle exit and the differentiation to monocytes [35,36]. But they also have an anti-proliferative function in the self-renewal capacity of mature macrophages, as MafB can directly bind and inhibit Ets-1 [37].
The mechanistic target of rapamycin (mTOR) is another downstream target of CSF1. It senses and integrates environmental stimuli and promotes cell growth and metabolism. Activation of mTORC1 in macrophages results in degradation of the cell cycle inhibitor $p27^{Kip1}$ and expression of cyclins A and D [38]. Additionally, mTORC1 is also responsible for the G2/M DNA damage checkpoint recovery, which is important for the progression of the cell cycle after DNA damage [39]. The work of Hsieh et al. also showed that inhibition of mTORC1 resulted in a decrease of mitotic cells, therefore is an important upstream regulator of the cell cycle in macrophages [39].

1.4 Peritoneal macrophages

The peritoneal cavity is a unique compartment with many different types of immune cells and many studies on the cells drawn from the peritoneal cavity helped to increase the knowledge about macrophage biology. For instance the labelling experiments performed by van Furth and Cohn [3].
Flow cytometry analysis showed that different immune cell subsets reside in the peritoneal cavity. The most abundant cell type in the peritoneal cavity are B-cells with approximately 40%. Among the rest, 55% are peritoneal macrophages, 35% T-, NK- and NKT-cells. The remaining 10% consists of neutrophils and eosinophils. Among peritoneal macrophages, the majority, 90%, are large peritoneal macrophages (LPM), whereas only 10% are comprised of small peritoneal macrophages (SPM) [40].

1.4.1 Phenotypic differentiation of peritoneal macrophages

The two subsets of peritoneal macrophages can not only be distinguished by their size, but also by the expression of typical macrophage surface markers. LPMs can be characterized by high expression of CD11b and F4/80. SPMs, on the other hand, express 3 times less CD11b and 80 times less F4/80 compared to LPMs. However, SPMs show an upregulated MHC-II expression, whereas LPMs do not [40].

1.4.2 Origin

Although both peritoneal macrophage subtypes display a phagocytic activity, they use different strategies. However, a *in vivo* phagocytosis assay with GFP-labelled bacteria showed that phagocytosis was more efficient in SPMs compared to LPMs [40]. Additionally, their response to an *in vivo* challenge with supernatant containing bacterial products differed drastically, as SPMs secreted high levels of NO and pro-inflammatory cytokines like IL-1β, IL-1α, TNF-α and IL-12. In contrast, LPMs produced GM-CSF and IL-10 (anti-inflammatory profile) [41]. This could be due to their different origin, as monocytes, recruited to inflammatory lesions, often display a pro-inflammatory profile [42]. Also with the recent discovery of a prenatal origin of tissue-resident macrophages, the dynamics of recruitment and maintenance of peritoneal macrophages was revisited.
Under steady state conditions, neither LPM nor SPM can be detected in the blood or any other tissue. However, CD62L, an adhesion molecule, is expressed on about half of SPMs, which where shown to migrate to lymphoid tissue after stimulation [40]. Cain et al. showed that LPMs, in contrast to short lived SPMs, share a more distantly related progenitor, validating an origin from the yolk sac [43]. SPMs on the other hand, originate from circulating monocytes (Ly6c^{hi} MHCII^{-}), which expression profile shifts with time to a more typical SPM phenotype (Ly6c^{-} MHCII^{hi}) [40].
Studies from the 80ies showed that peritoneal macrophages have the capacity to maintain themselves through self-renewal [44]. These data combined with the analysis of the cell cycle and DNA content showed, that LPMs are maintained at a low-level proliferation under steady state conditions in adult mice, but undergo a proliferative burst after acute inflammation. SPMs, however, are rather short-lived and show no proliferative capacity

under steady state or inflammatory conditions [45].

1.4.3 Macrophage disappearance reaction

The macrophage disappearance reaction in the peritoneal cavity is associated with adherence of macrophages to the structural tissue lining the intestines (omentum), emigration to draining lymph nodes, into visceral organs such as liver or spleen, or even cell death [46, 47]. In case of inflammatory stimuli, LPMs disappear from the peritoneal cavity via migration to the omentum [47–49] and SPM and monocyte numbers increase [40]. This contributes to the capacity of the peritoneal cavity to handle infections and inflammatory stimuli, as SPMs develop a pro-inflammatory profile in the course of inflammation and produces high levels of e.g. TNF-α. LPMs, on the other hand, appear to develop a M2 polarization profile and are important for tissue homeostasis of the peritoneal cavity after inflammation [40, 43, 45].

1.5 Cell cycle and Cell cycle kinases

Cell division is a highly regulated process. Two classes of proteins are responsible for the progression through the cell cycle: Cyclin-dependent kinases (Cdks) and Cyclins [50]. They form a heterodimeric serine/threonine protein kinase. Cdks form the catalytic subunit of this heterodimeric complex and require binding of cyclins, the regulatory subunit [51]. These are synthesised and degraded during the cell cycle in a cyclic fashion. The first Cdk, Cdc2, was discovered 1980 in yeast. It was shown to be essential and solely responsible for cell-cycle progression in yeast [52]. A few years later the human homolog of Cdc2 was found [53] and later named Cdk1.
So far 21 different Cdks and about 30 cyclins were identified in mammalian cells, which can be classified in two subfamilies: cell-cycle-related and transcriptional Cdks [54–56].

1.5.1 The Cell Cycle

In the past 10 years a cell-cycle model was created through extensive research. According to this 'classical' model, cells after cytokinesis can either chose to stop proliferating, a phase called quiescence (G0), or continue to divide. In the latter the cells advance to the G1 phase, which is highly regulated. Synthesis of D-type cyclins is induced by mitogenic signaling, followed by the binding and transport of Cdk4 and Cdk6 to the nucleus. This active Cdk/cyclin complex phosphorylates members of the retinoblastoma (Rb) protein family. Rb proteins are repressors of transcription, as they bind and inhibit the activity of transcription factors, such as the E2F family. One of the most crucial targets of E2F are E-type cyclins, which are required at later stages of the cell cycle [57, 58].
Despite the initial phosphorylation of Rb proteins carried out by either Cdk4/Cyclin D or Cdk6/Cyclin D, irreversible inactivation of this protein family is mediated by Cdk2-Cyclin E, which leads to activation of transcription factors, chromatin remodelling complexes, histone deacetylases and other necessary genes important for the subsequent phases of the cell cycle, such as genes encoding A-type and B-type cyclins. From this point on, no mitogenic signals are required to undergo cell division (restriction point) [59].
But the Cdk2/Cyclin E complex is not only responsible for the inactivation of Rb proteins, but also essential for the entry into S-phase and the initiation of DNA replication [60]. Thereafter, this complex is silenced by a rapid degradation of Cyclin E to avoid re-replication of DNA [61, 62].
Once Cyclin E is not associated with Cdk2, A-type cyclins, accumulating during S-phase, bind to Cdk2 and together mediate phosphorylation of proteins required for the completion and exit from S-phase, including transcription factors, DNA replication and repair proteins and upstream regulators of Cyclin A [63, 64].
At the end of S-phase and the beginning of G2-phase, Cyclin A dissociates from Cdk2 and binds to Cdk1. However not much is known about the role of the Cdk1/Cyclin A complex and how it is differing from Cdk2/Cyclin A. Only Koseoglu et al. showed, that this complex is responsible for the inhibition of histone mRNA biosynthesis, in order to prevent histone accumulation [65]. During G2, A-type cyclins are degraded and B-type cyclins are synthesised and form a complex with Cdk1, which is important for the progression through mitosis. This complex not only associates with centrosomes, but also mediates different structural and regulatory processes, such as chromosomal condensation, disassembly of the Golgi apparatus [66, 67] and breakdown of nuclear

lamins [68]. Exit from mitosis is mediated by the inactivation of the Cdk1/CyclinB complex by degradation of B-type cyclins, which is regulated by the anaphase-promoting complex [69, 70].

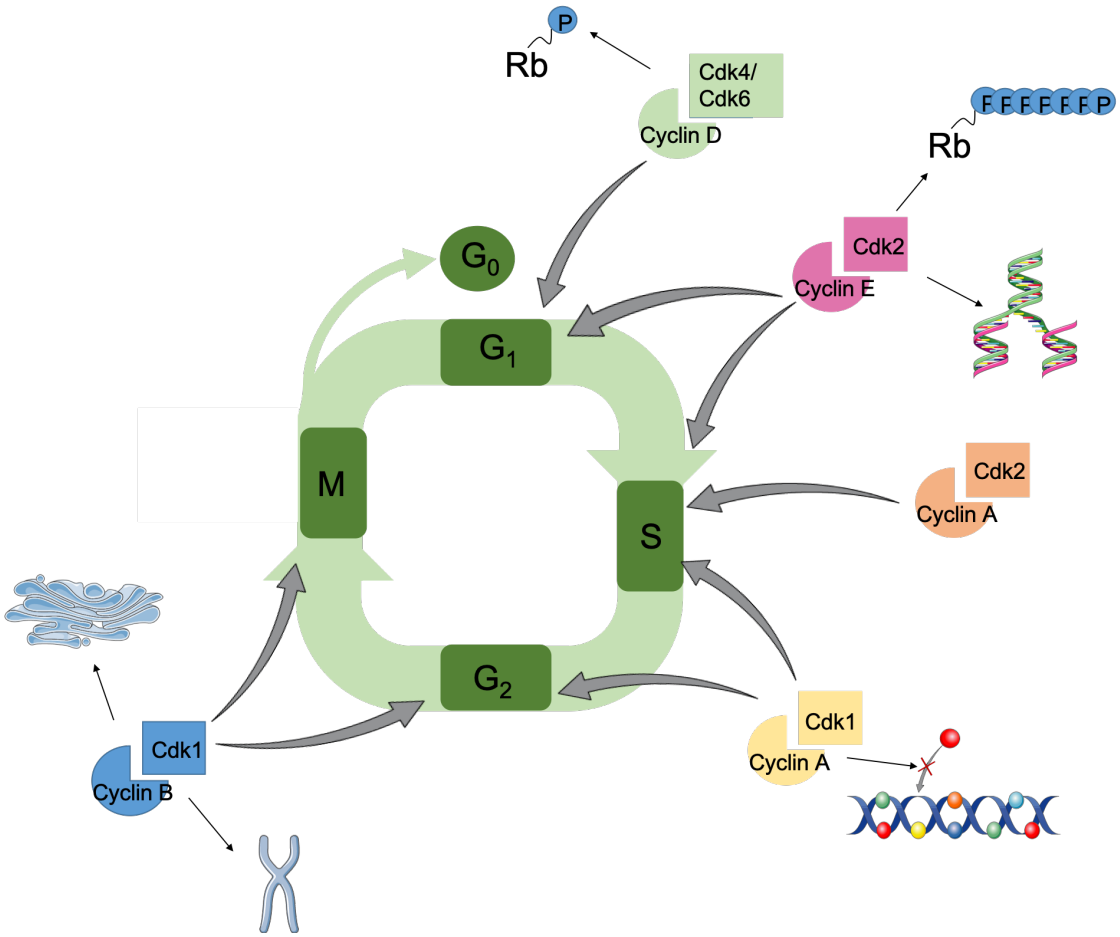

Figure 2: **Cdk-Cyclin complexes in the mammalian cell cycle.** For further details see text.

1.5.2 Cyclin-dependent kinases and their role in mammalian development

As previously mentioned, the mammalian genome contains at least 20 different Cdks, however there has been reported a widespread compensation among Cdks and cyclins. There are, for instance, mouse knock-outs of Cdk2 [71, 72], Cdk4 [73] or Cdk6 [74] viable, which indicates that those interphase Cdks are not essential for the cell cycle of most cell types. However, each of those Cdks can cause developmental defects in specialised cells [72–74]. For instance, experiments performed on mouse models showed that the loss of Cdk4 in mice results in diabetes and defect in the proliferation of endocrine cells (pancreatic β-cells or pituitary hormone-producing cells) [73]. Minor proliferative defects are recognised in cells of the erythroid lineage in Cdk2$^{-/-}$ Cdk6$^{-/-}$ and Cdk4$^{-/-}$ Cdk6$^{-/-}$mice were shown to be sterile due to defects in meiosis, but had no detectable mitotic defects [75]. Also Cdk2$^{-/-}$ Cdk4$^{-/-}$ are embryonic lethal, due to the accumulation of hyperphosphorylated Rb protein [76].
Interestingly, there are no full Cdk1 knock-out mice viable, which suggests an embryonic lethality of these mutant mice due to a cell cycle arrest at the two-cell stage. The fact, that there are no defects in the cell cycle detectable in the absence of interphase Cdks, except from highly specialised cells, can be explained by the compensatory role of Cdk1. However, Cdk1 cannot be compensated by other Cdks, which makes Cdk1 the only essential Cdk for the progression through the cell cycle in most cell types [50,77,78].

1.6 Objective

Cdk1 plays an essential role in the cell-cycle progression. Previously, mouse knock-outs of other cyclin-dependent kinases were used to elucidate the mechanism behind the cell cycle. However full knock-out mice of Cdk1 are embryonically lethal and thus not viable due to a cell cycle arrest at the two-cell stage [78]. Macrophages play a central role in the initiation of innate and adaptive immunity, maintenance of tissue homeostasis and its recovery after injury. To achieve this maintenance and clearance of pathogens, macrophages need to proliferate, which is not fully understood until now. In order to address and overcome the problem of embryonic lethality, we used conditional knock out mice specifically targeting the ablation of Cdk1 expression in myeloid cells. As macrophage proliferation can either have beneficial or disadvantageous effects on the outcome of certain inflammatory and non-inflammatory conditions, the identification of the role of Cdk1 in the cell cycle and in the proliferation of macrophages might identify new treatment strategies.

2 Materials and Methods

2.1 Mice

Cdk1$^{fl/fl}$ mice were crossed to LysM$^{cre/+}$ mice to obtain Cdk1$^{fl/fl}$ $LysM^{cre/+}$ and Cdk1$^{fl/fl}$ $LysM^{cre/cre}$ mice respectively. Spleen, liver, lung and brain were isolated and fixed for histology, femur, tibia and humerus were used for bone marrow isolation.

2.2 Cell Culture

If not indicated otherwise, cells were cultured at 37°C in a humidified CO_2 (5%) incubator (Thermo Scientific Heraeus Incubator BBD 6220).

2.2.1 Media and Buffers

Macrophage Differentiation Medium

- Dulbecco's modified Eagle's medium with 4.5 g/l D-Glucose and 0.11 g/l Sodium Pyruvate (Gibco)
- 10% Fetal Bovine Serum (FBS), low endotoxin (Sigma Aldrich)
- 2 mM L-Glutamine (Lonza)
- 60 mg/l Penicillin (Sigma)
- 100 mg/l Streptomycin (Sigma)
- 50 nM β-Mercaptoethanol (Gibco)

FACS Buffer

- Dulbecco's phosphate-buffered saline w/o Ca^{2+} and Mg^{2+}
- 2% FBS, HI, low endotoxin (Gibco)
- 2 mM Ethylenediaminetetraacetic acid (EDTA)

10× *Red Blood Cell (RBC) Lysis Buffer*

- 82.6 g Ammonium chloride
- 10 g Potassium bicarbonate
- 0.37 g EDTA
- filled up to 1 l with ddH_2O
- sterile filtered, pH adjusted to 7.3 with HCl

2.2.2 Bone Marrow Derived Macrophage Differentiation

Femur, tibia and humerus were isolated completely intact from mice. Bones were freed from muscle tissue and washed first in 70% Ethanol and sterile DPBS. Both epiphyses were removed to open the bones. A 27 G needle (BD Microlance 3) was inserted at one end and bone marrow cells were flushed with Macrophage (Mϕ) Differentiation Medium. Bone Marrow cells were seeded in 10cm non-treated cell culture dishes and supplemented with 20 ng/ml M-CSF (Peprotech). For the whole bone marrow 5 plates were used containing each 8 ml differentiation medium. After three days, cells were washed with DPBS to remove non-adherent cells, new differentiation medium supplemented with 15 ng/ml was added, attached cells were scraped off the bottom with a Cell Scraper (Cyto One) and split 1:2. On day 5, 5 ng/ml M-CSF was added to the cells. The next day, fully differentiated cells were washed and harvested using a Cell Scraper, counted and seeded for experiments at different concentrations.

2.3 Isolation of Peritoneal Macrophages

To isolate macrophages from the peritoneal cavity, 10 ml of ice cold DPBS was injected into the peritoneum carefully using a 27 G needle. The abdomen was massaged to dislodge any attached cells and the fluid was collected using a 20 G needle. The collected cell suspension was centrifuged for five minutes at 350g (4°C), the pellet resuspended in 1 ml 1× RBC Lysis Buffer and incubated for two minutes at room temperature. To inactivate the Lysis Buffer, 9 ml 2% FCS in DPBS was added. The cell suspension was counted and a defined amount of cells used or seeded for further experiments.

2.4 Macrophage Isolation from Lung Tissue

Digestion Mix (20 ml)

- 5% FBS
- 200 μl CollagenaseD
- 3.11 μl DNase I
- filled up to 20 ml with HBSS

Isolation Buffer

- 5% FBS
- 2 mM EDTA
- HBSS

Lung lobes were isolated from the mouse, placed in 500μl ice cold digestion mix and cut into small fragments. A volume of 600μl pre-warmed digestion mix was added and the sample incubated for 30 minutes at 37°C 300rpm. Tissue was strained trough a 70μm cell strainer (Corning) and washed with isolation buffer. Samples were centrifuged for 10 minutes at 4°C 300g prior to lysing the pellet with 2 ml of ACK Erythrolyse. After another centrifugation step, the pellet was resuspended in FACS Buffer, cell were counted and prepared for further analysis.

2.5 Flow Cytometry

Flow cytometric analysis was performed with BMDMs, peritoneal macrophages (for panel see Table 2) and lung tissue (for panel see Table 1). If not indicated otherwise, all steps were performed on ice and all centrifugations at 350g on 4°C. Shortly, cells were washed with FACS Buffer, blocked 10 minutes with 1μl/ 1×10^6 cells TrueStain FcR (BioLegend) and stained for 20 minutes in the dark. Cells were washed twice with FACS Buffer prior to labeling with 50μg/ml Live/Dead marker 7AAd. The stainings were acquired using a Cytoflex S (Beckman Coulter) and analysed with FlowJo.

Table 1: Panel for Analysis of Lung Macrophages

Specificity	Fluorophore	Dilution	Company	Cat.Nr.
CD45.2	AF488	1:300	Biolegend	109816
CD11c	PE-Cy7	1:350	eBioscience	25-0114-81
MHC II	BV605	1:300	BD Biosciences	563413
CD11b	eF450	1:300	eBiosciences	48-0112-82
Siglec F	PE	1:300	BD Biosciences	562068
CD103	AF700	1:200	eBioscience	56-1031-82
Ly6C	APC-Cy7	1:200	BD Biosciences	560596
Ly6G	PerCP-Cy5.5	1:200	BioLegend	127615
CD64	APC	1:200	BioLegend	139306
CD24	BV510	1:200	BioLegend	101831

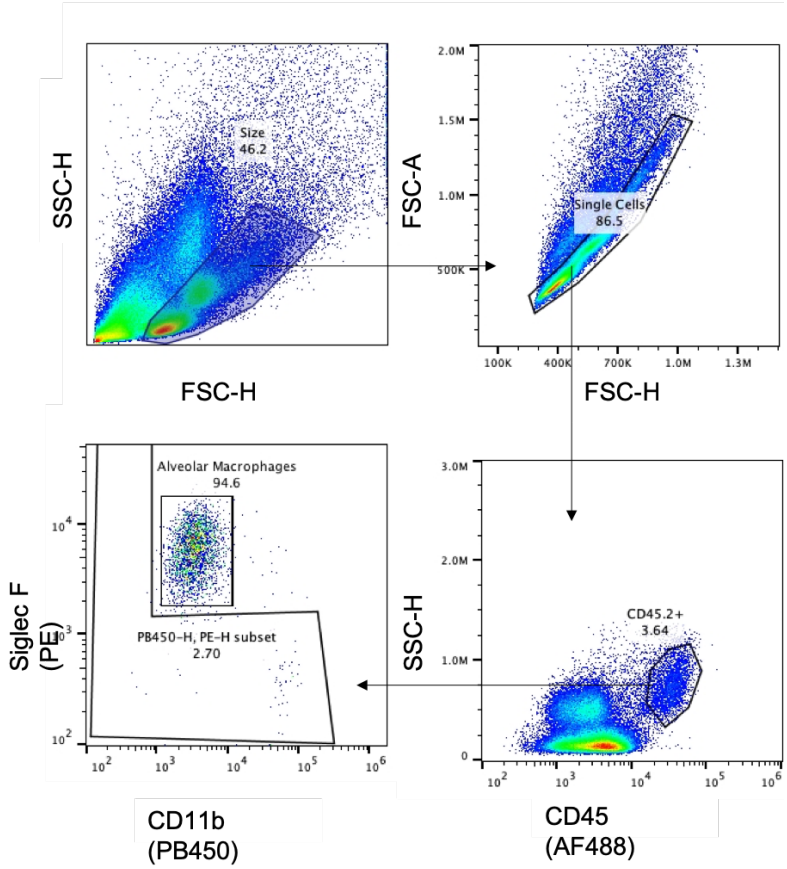

Figure 3: **Gating strategy for alveolar macrophages**

Table 2: Panel for Analysis of Peritoneal Macrophages

Specificity	Fluorophore	Dilution	Company	Cat.Nr.
F4/80	APC	1:100	Biolegend	123116
CD11b	eF450	1:100	eBioscience	48-0112-82
CD115	FITC	1:100	eBioscience	53-1152-82
Ly6G	PerCP-Cy5.5	1:100	BioLegend	127615

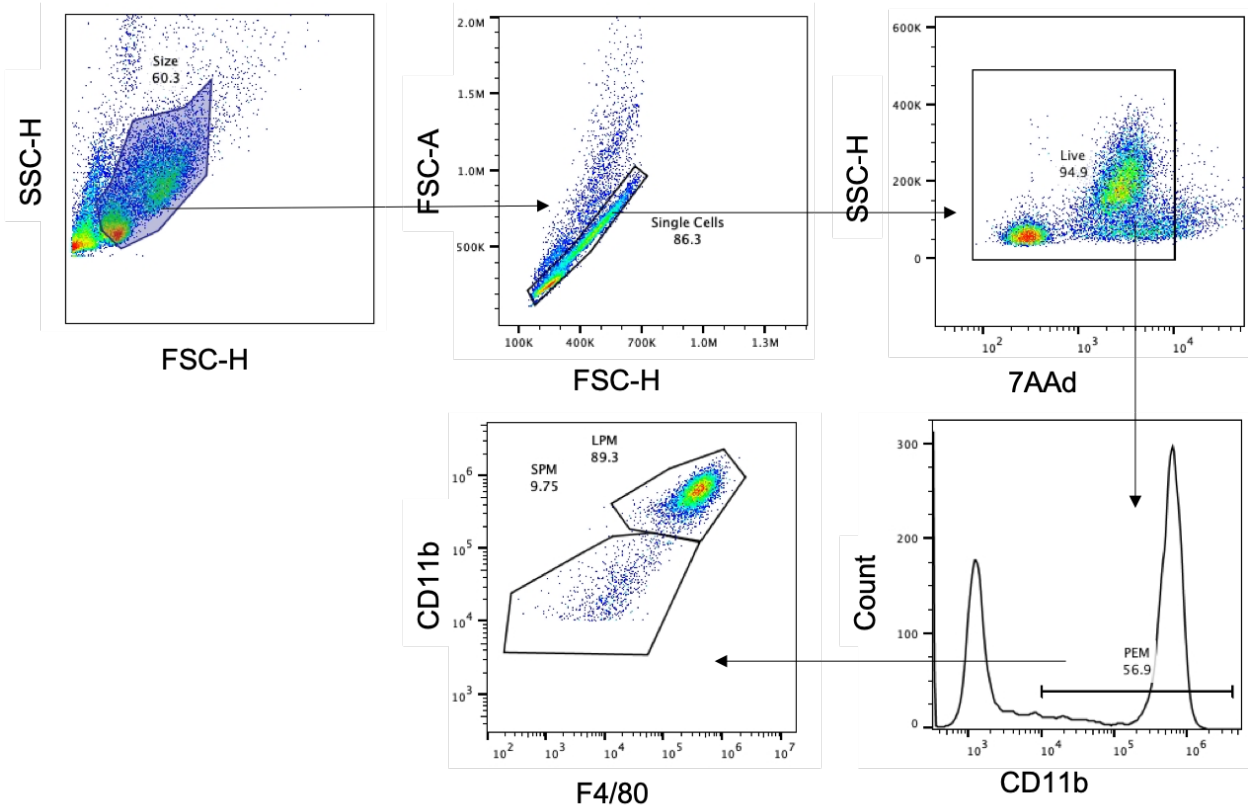

Figure 4: **Gating strategy for peritoneal macrophages**

2.5.1 EdU Proliferation Assay

1×10^6 cells were seeded in a 6-well non-treated tissue culture plate. After one hour half of the medium was replaced with fresh differentiation medium containing EdU with an end concentration of 10 μM. Cells were replaced in the incubator and after two hours washed with DPBS and harvested. After centrifugation for five minutes at 350g at 4°C, cells were washed once with 1%BSA in DPBS and centrifuged for 5 minutes at 10000rpm at 4°C. Cold (-20°C) Methanol was added to the pellet to fix and permeabilise the cells. After 10 minutes of incubation at -20°C, the cell suspension was centrifuged, the supernatent discarded and the pellet washed two times with 1%BSA in DPBS. The Click-iT® reaction cocktail was prepared (according to Table 3) and 125 μl was added to the pellet and incubated light protected at room temperature. After 30 minutes the cells were washed with 1%BSA in DPBS and stained light protected with 125 μl RNase(8 μg/ml) and 7-AAD (400μg/ml) for 30 minutes at room temperature, prior to a final washing step with FACS Buffer (2% FCS HI and 2 mM EDTA in DPBS). Samples were recorded on a Cytoflex S.

Table 3: EdU Click-iT® reaction cocktail

Components	Number of reactions						
	1	2	5	10	15	30	50
DPBS	108.75 μl	217.5 μl	543.75 μl	1.09 ml	1.63 ml	3.26 ml	5.44 ml
$CuSO_4$	2.5 μl	5 μl	12.5 μl	25 μl	37.5 μl	75 μl	125 μl
Fluorescent dye azide	1.25 μl	2.5 μl	6.25 μl	12.5 μl	18.75 μl	37.5 μl	62.5 μl
1x Reaction Buffer Additive	12.5 μl	25 μl	62.5 μl	125 μl	187.5 μl	375 μl	625 μl
Total Volume	125μl	250 μl	625 μl	1.25 ml	1.88 ml	3.75 ml	6.25 ml

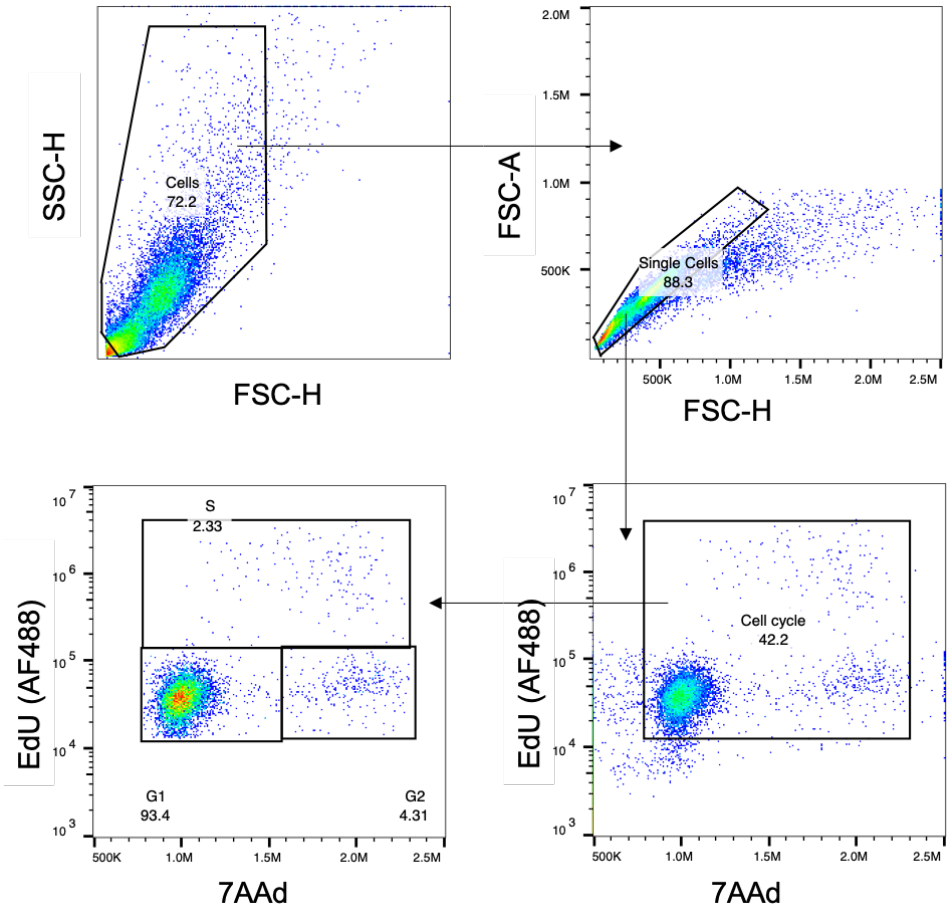

Figure 5: **Gating strategy for proliferation assay**

2.6 Histology

Mouse tissue was fixed overnight in 4% Roti-Histofix (Roth) at 4°C, washed twice in DPBS and transferred in 70% EtOH (Merck) for storage. The tissue was dehydrated to allow infiltration of the tissue by paraffin in a series of Isopropanol (Roth) solutions (80% Isopropanol, 90% Isopropanol and 100% Isopropanol, each 1h). The tissues were then transferred to molten paraffin and incubated for 2 and 3 hours. The tissues were embedded in paraffin. Paraffin-blocks were cut into 3μm sections with a microtome, mounted onto Superfrost Plus microscope slides (Thermo Scientific) and used for histological stainings.

2.6.1 Immunohistochemistry

3μm tissue section were incubated for 1 hour at 60°C, deparaffinized and rehydrate in a series of washes: Xylene 1 (10 minutes), Xylene 2 (10 minutes), Isopropanol (10 minutes), 96% EtOH (10 minutes), 70% EtOH (5 minutes), 50% EtOH (5 minutes) and three times in PBS (each 3 minutes). Antigen retrieval was done with either 10x Tris-EDTA solution (10mM Tris, 1mM EDTA, 0.05% Tween 20) for brain tissue or 10x Target Retrieval Solution, Citrate pH6.1 (Dako). To avoid non-specific binding, slides were treated with 1% H_2O_2 for 10 minutes to inhibit endogenous HRP enzymes. Next, they were immersed 5 minutes in 0.1% Triton-X100 (Sigma Aldrich) prior to blocking 20 minutes in 2.5% horse serum. Subsequently, about 150μl diluted primary antibody (see Table 4) was pipetted on the tissue and incubated overnight on 4°C in a wet chamber. The next day, tissues were coated with diluted secondary antibody(see Table 4). After 45 minutes of incubation at room temperature, slides were washed and immersed 30 minutes with Novocastra Streptavidin-HRP (Leica), followed by AEC-high sensitivity substrate chromogen (Dako). Counterstaining was performed using Mayer's Hemalum Solution (Merck) and slides were mounted with Aquatex (Merck).

Table 4: List of Antibodies used for IHC

Specificity	**Host Species**	**Company**	**Final Dilution**
F4/80	rat		1:800
Tmem119	rabbit		1:1000
anit-rat	goat		1:500
anti-rabbit	horse		1:500

2.7 RNA Isolation

All steps were performed on ice and all centrifugations were done at 12.000g 4°C with a microcentrifuge. Bone marrow derived macrophages were seeded in a 12 well-plate at a density of 1×10^6/ml. After 6 hours, cells were washed with DPBS, 500 μl TRI®-Reagent (Sigma-Aldrich) was added to the cells and frozen at -80°C for at least 12 hours. Cells in TRI®-Reagent were transferred to a chloroform-water solution, mixed and incubated for 10 minutes. After centrifugation for 15 minutes, the aqueous phase was transferred to a new Eppendorf tube containing Isopropanol and Glycan Blue and incubated for 30 minutes, prior to centrifuging the samples for 30 minutes. The supernatant was discarded completely and 1ml 75% EtOH to wash the RNA was added and centrifuged for 7 minutes. This step was repeated again, the supernatant discarded completely and the pellet air-dried for about 10 minutes. The pellet was resupendend in 10 μl nuclease free water and the concentration measured on Nanodrop.
Reverse Transcription was performed to generate cDNA from the RNA samples. For the synthesis, the RNA concentrations were adjusted to the least concentrated sample. The GoScript^{TM} Reverse Transcription kit (Promega) was used, with a reaction volume of 20 μl, where 5 μl isolated RNA, 5 μl nuclease free water was added to 10 μl 10× master mix containing 2 μl GoScript Enzyme, 4 μl GoScript Buffer and 4 μl nuclease free water. After completing the cDNA program (25°C for 5 min, 42°C for 1 h and 70°C for 15 min), the resulting cDNA was diluted 1:10 with nuclease free water and used for quantitative real-time PCR.

2.8 Quantitative Real Time PCR

All primers were designed with the NCBI Primer-BLAST tool and reconstituted with nuclease free water to a concentration of 100pmol/μl.

Table 5: List of Primers used

Oligoname	**Sequenze**	**TM** [°C]	**GC-content** [%]
CDK1 ctrl fwd	GTACACACACGAGGTAG	59.8	52.4
CDK1 ctrl rev	GTCAACCGGAGTGGAGT	59.4	55
CDK1 fwd	AGAGAGGGTCCGTCGTA	58.8	57.9
CDK1 rev	ACCTTATACACCACACC	57.3	50
β-actin fwd	CACACCCGCCACCAGTTCGC		
β-actin rev	TTGCACATGCCGGAGCCGTT		

Quantitative Real Time PCR was performed using the SYBR Green based GoTaq® qPCR Master Mix (Promega) on a StepOnePlus^{TM} Real-Time PCR System (Bio-Rad). In one reaction volume of 10 μl, 2 μl cDNA, 5 μl 2× GoTaq® Master- Mix, 2.96 μl nuclease free water and 0.02 μl per primer (forward and reverse). All samples were measured in duplicates, the mRNA expression levels were normalized to β-actin mRNA expression, and further normalized to the average expression of the control group.

2.9 Western Blot

2.9.1 Media and Buffers

PIM (1 ml)

- 200 μg Leupeptin
- 200 μg Aprotinin
- 30 μg Benzomidinchloride
- 1 Trypsininhibitor
- 0.5 mM Na_3VO_4
- 0.5 mM DTT

Buffer A

- 20 mM Hepes, pH 7.9
- 0.4 M NaCl
- 25% (v/v) Glycerin
- 1 mM EDTA
- 0.5 mM Na_3VO_4
- 0.5 mM DTT

WB Lysis Buffer (1 ml)

- 830 μl Buffer A
- 40 μl PIM
- 20 μl 100 mM PMSF
- 100 μl 10×Protease Inhibitor (Roche)
- 10 μl Triton X-100

10× *Tris-buffered saline (TBS)*

- 1.5 M NaCl
- 0.5 M Tris, pH 7.4

1× *TBS/Triton X-100 (TBS-T)*

- 1:10 10×TBS
- 1:1000 Triton X-100

4× *SDS Loading Dye*

- 200 mM Tris, pH 6.8
- 1 M DTT
- 8% (w/v) SDS
- 0.4% (w/v) Bromophenol blue
- 40% v/v Glycerol

10× *Electrophoresis Buffer*

- 60.6 g Tris
- 292 g Glycine
- 100 ml 20% (w/v) SDS
- filled up to 2 l with ddH_2O

Harlow Buffer

- 29 g Tris
- 145 g Glycine
- 25 ml 20% (w/v) SDS
- 1 l MeOH
- filled up to 5 l with ddH_2O

2.9.2 Cell Lysis

Approximately 2×10^{6} BMDMs were seeded in 6-well plates with differentiation medium over night. The wells were washed with PBS and the macrophages harvested in 1 ml PBS/2% FCS with a Cell Scraper. After 5 minutes of centrifugation with 500g, all supernatant was discarded and the cell pellet resuspended in 50-70 μl WB Lysis Buffer, depending on the pellet size. The suspension was kept on ice for 20 minutes with 2 short interruptions, where the pellet was frozen in liquid nitrogen to improve cell lysis. After 15 minutes centrifugation at 14.000g the supernatant was collected.
The protein content was determined with the Bradford Assay. Exactly 1 μl of sample was added to 1 ml of Bradford reagent (BioRad Protein Assay), followed by a 15 minute incubation in the dark prior to measuring the protein content.
The protein concentrations were adjusted to 15 μg with WB Lysis Buffer, mixed with 4× SDS Loading Dye, heated to 95°C for 5 minutes and stored at -80°C.

2.9.3 Immunoblotting

The sample volume of 12 μl (corresponding to 15 μg of total protein was loaded on a 10% polyacrylamide gel (see Table 6). The proteins were separated with 110V for about 90 minutes and the transfer onto a nitrocellulose membrane was performed in cold Harlow Buffer at 350 mA for 1 hour.

Table 6: Recipe for a 10% Polyacrylamide Gel

Reagent	**Stacking Gel**	**Separation Gel**
30% AA/Bis (BioRad)	1.33 ml	3.33 ml
0.5 M Tris-HCl, pH 6.8	2.5 ml	-
1.5 M Tris-HCl, pH 8.8	-	2.5 ml
10% SDS	100 μl	100 μl
ddH_2O	6.07 ml	4.07 ml
TEMED (BioRad)	10μl	10μl
10% APS (Amersham)	100μl	100μl

After the transfer, the membrane was washed in distilled water and stained with PonceauS, cut at the desired fragment size and washed three times in TBS-T to remove the staining. Unspecific antibody binding sites were blocked for 1 hour at room temperature in TBS-T/4% skim milk powder prior to the over night incubation at 4∘C in the respective primary antibodies (prepared in TBS-T/5% BSA/0.02% NaN_3).
The membrane was washed three times in TBS-T, followed by 1 hour incubation with the corresponding secondary antibodies (diluted in TBS-T/4% skim milk powder) at room temperature. The signals were detected after washing three times with TBS-T using an Odyssey CLx imager (LI-COR).

Table 7: List of Antibodies used for WB

Specificity	**Host Species**	**Company**	**Dilution**
α-tubuline	mouse	Cell Signaling Technologies	1:1000
Cdk1	mouse	Santa Cruz Biotechnology	1:200
mouse IgG	goat	LI-COR	1:15000

3 Results

3.1 Deficiency of Cdk1 expression has no effect on macrophage proliferation in Cdk1$^{fl/fl}$LysM$^{cre/+}$ mice

3.1.1 Mouse model

As a complete knock out of Cdk1 leads to embryonic lethality, we generated mice with a deficiency of Cdk1 expression specifically in myeloid cells. For this reason, mice with LoxP sites flanking exon 3 in the Cdk1 locus [78] were crossed with mice carrying the cre recombinase under the influence of the Lysozyme M (LysM) promotor [79], which is only active in myeloid cells. Therefore, Cdk1 is truncated upon cre expression in macrophages and neutrophils of Cdk1$^{fl/fl}$LysM$^{cre/+}$ mice (wild-type mice are in the following described as Cdk1$^{fl/fl}$LysM$^{+/+}$).

3.1.2 Deficiency of cell proliferation in Bone Marrow derived Macrophages (BMDM)

We isolated and differentiated bone marrow from Cdk1$^{fl/fl}$LysM$^{cre/+}$ mice and determined the cell number to see, if proliferation was impaired in the cre/+ BMDMs. At day 6 there were less cells from knock-out mice compared to wild-type mice. Cells of the Cdk1 knock out mice had a round shape, whereas wild-type macrophages were more stretched out (Fig.6A). Additionally, the counted cell number showed a slight decrease in knock-out mice, however this result was not significant (p=0.09) (Fig.6B). As Cdk1 plays an important role in progression through the cell cycle and cell proliferation, these slightly reduced cell numbers argue for a decreased proliferation rate in Cdk1 knock-out mice. However, the cell numbers were not reduced significantly, which could be due to an insufficient knock out of Cdk1.

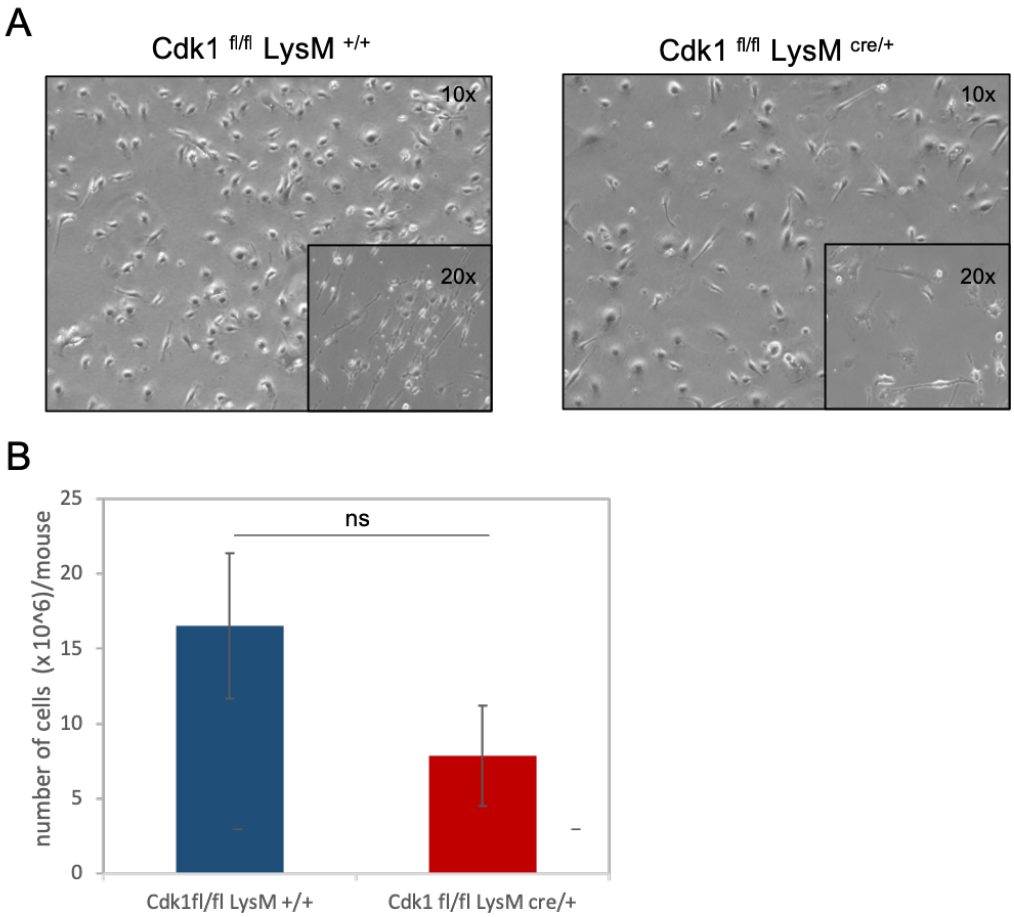

Figure 6: **Slightly decreased cell numbers of BMDM.** (**A**) Photos of BMDM at day 6. (**B**) Number of cells counted after 6 days of differentiation with a Hemocytometer. Shown is the average of n=3, with the error bars representing SD.

3.1.3 Cdk1 knock-out in BMDM

To see, if Cdk1 was deleted properly, quantitative Real-Time PCR with primer binding to the Cdk1 locus was performed. There were two different primer pairs used, to quantify the Cdk1 deletion (Fig.7A). One primer pair was generated as a control for the background levels of Cdk1, whereas the other pair determines the actual quantity of Cdk1. To achieve this, we generated the reverse primer to bind to exon 3, which is absent in Cdk1 $^{fl/fl}$ LysM $^{cre/+}$ mice. Therefore, no signal is detectable for this primer pair. The Cdk1 control primer pair, on the other hand, was generated to bind to a short region in exon 4 and should be detectable in BMDMs in both Cdk1 $^{fl/fl}$ LysM $^{+/+}$ and Cdk1 $^{fl/fl}$ LysM $^{cre/+}$. After normalization of both to β-actin, we normalized the Cdk1 mRNA to the control mRNA and determined the difference between Cdk1 mRNA expression of Cdk1 $^{fl/fl}$ LysM $^{+/+}$ and Cdk1 $^{fl/fl}$ LysM $^{+/+}$ BMDMs.However, there was no change (p=0.7) of mRNA expression visible in Cdk1 $^{fl/fl}$ LysM $^{cre/+}$ BMDMs compared to Cdk1 $^{fl/fl}$ LysM $^{+/+}$ (Fig.7B).

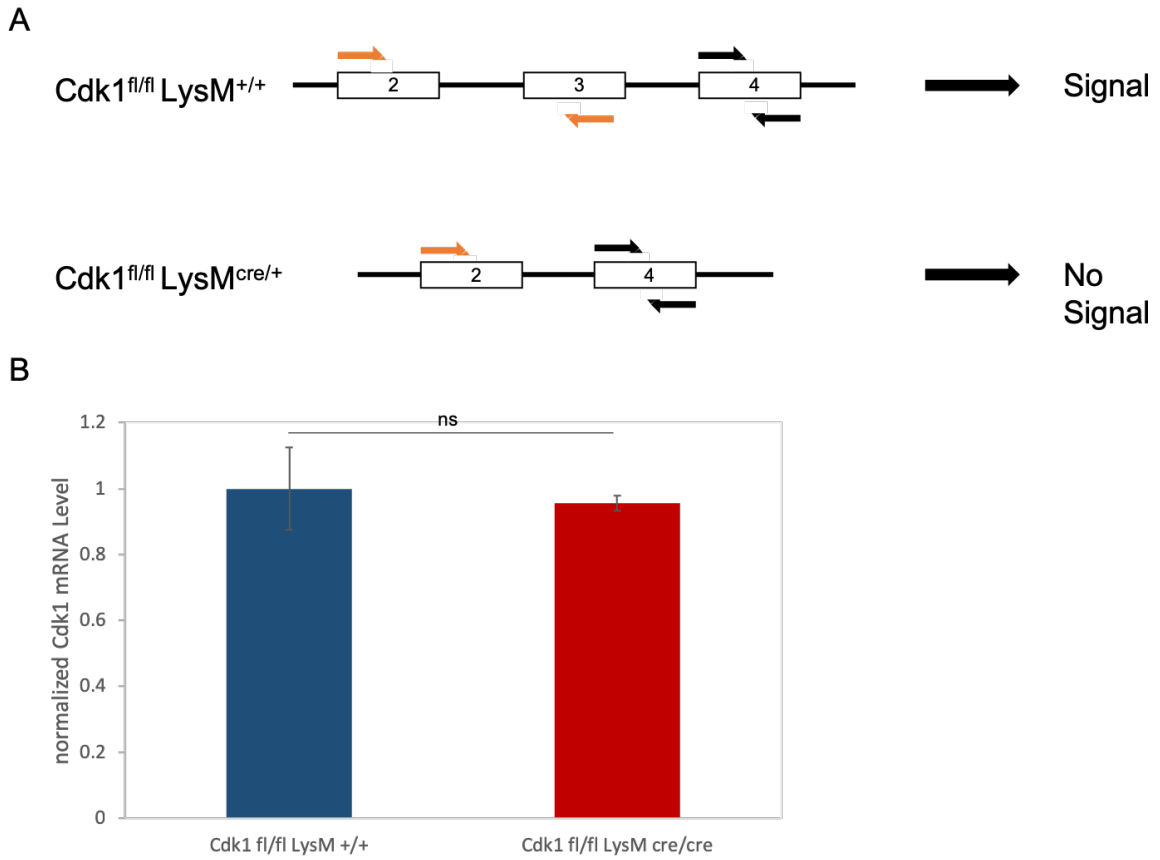

Figure 7: **Quantitative Real-Time PCR in Cdk1 $^{fl/fl}$ LysM $^{cre/+}$ BMDM shows no change in Cdk1 mRNA expression.**(**A**) Two different primer pairs were designed against the Cdk1 locus in mice for qPCR: A primer pair quantifying the background levels of Cdk1 (black arrows) and a primer pair quantifying the actual Cdk1 mRNA expression (orange arrows). For further details see text. (**B**) The expression of Cdk1 mRNA in BMDM, quantified by qPCR and normalized to β-actin and Cdk1 control. Graphs show the average Cdk1 levels of n=3, with the error bar representing the SD.

Additionally to mRNA expression, we tested the expression of Cdk1 protein by Western Blot Analysis in BMDM after 6 days of differentiation, where we saw only a slight decrease (p=0.23) of Cdk1 signal visible (Fig.8). Therefore, we concluded, that one cre-allele is not able to efficiently delete Cdk1.

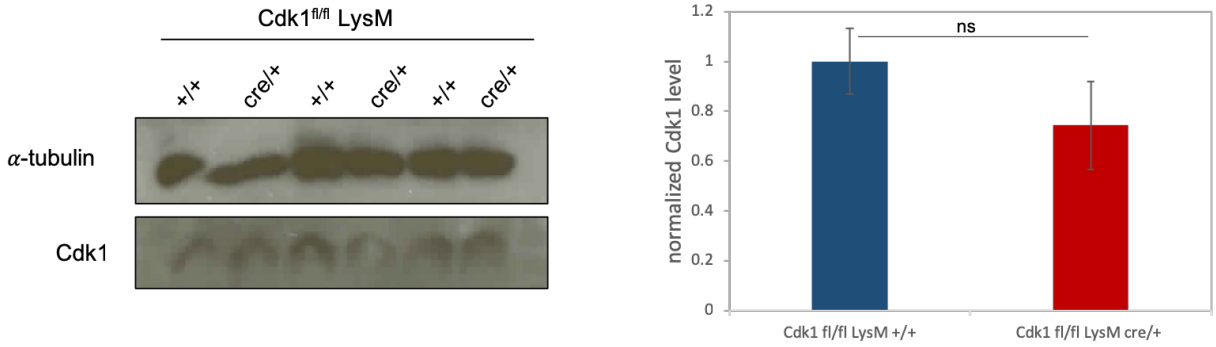

Figure 8: **Insufficient Cdk1 knock-out in BMDM (day6).** Cdk1 protein levels were quantified by western blot, and normalized to α-tubulin. The graphs show the average Cdk1 levels of n=3, with the error bar representing the SD.

3.2 Cdk1 deficiency has a negative effect on macrophage proliferation in Cdk1$^{fl/fl}$LysM$^{cre/cre}$ mice

3.2.1 Mouse model

As the previous results showed an insufficient deletion of Cdk1 in BMDM from mice with a heterozygous cre recombinase allele, we generated a homozygous Cdk1 knock-out in myeloid cells by crossing Cdk1 $^{fl/fl}$ LysM $^{cre/+}$ mice with each other. Additionally, we used Egfr$^{fl/+}$ LysM $^{cre/cre}$ and Egfr $^{fl/+}$ LysM $^{cre/+}$ mice as controls.

3.2.2 Deficiency of cell proliferation in BMDMs from homozygous mice

To test for the ability of macrophages in Cdk1 $^{fl/fl}$ LysM $^{cre/cre}$ mice to proliferate, we isolated bone marrow. After 6 days of differentiation we determined the number of cells. Cdk1 $^{fl/fl}$ LysM $^{cre/cre}$ BMDMs were reduced by approximately 60% compared to Cdk1 $^{fl/fl}$ LysM $^{+/+}$ (p=0.00003) and the Egfr controls Egfr $^{fl/+}$ LysM$^{cre/+}$ and Egfr $^{fl//+}$ LysM $^{cre/cre}$ (p=0.0002 and p=0.004) (Fig.9A). Egfr $^{fl/+}$ LysM$^{cre/+}$ and Egfr $^{fl//+}$ LysM $^{cre/cre}$ were used to eliminate the possibility of the homozygous cre recombinase to be responsible for the reduction of BMDM, due to its proposed cytotoxic effects [80]. We also noticed bigger and more roundly shaped cells in the knock-out cells compared to the elongated cells in the wild-type (Fig.9B). These data suggest an impact of Cdk1 on the proliferative capacity of macrophages.

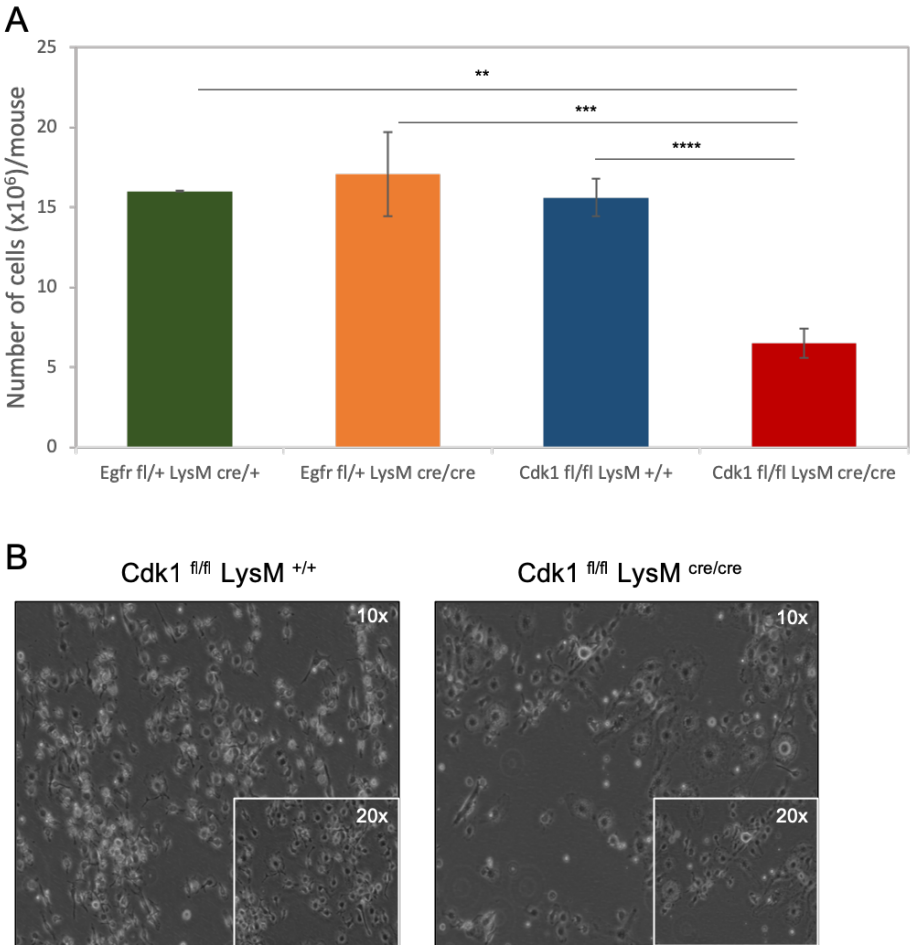

Figure 9: **Significantly reduced cell number of homozygous Cdk1 knock-out BMDMs.**(**A**) Number of cells counted after 6 days of differentiation with a Hemocytometer. The graphs show the average (n=3-9) number of cells per mouse, with the error bars representing the SD. (**B**) Photos of BMDMs taken at day 6.

3.2.3 Cell cycle analysis reveals a proliferative defect in the G2-M transition of Cdk1 $^{fl/fl}$ LysM $^{cre/cre}$ BMDM

As the Cdk1–Cyclin B complex is thought to regulate the G2–M transition and progression through mitosis, we wanted to have a closer look at the progression through the cell cycle. Therefore we performed an EdU/7AAd staining where we can differentiate between the 3 cell cycle phases G1, S and G2/M. In this experiment we noticed a significant increase of approximately 5-fold in the G2/M phase (p=0.0005) and about 3.5-fold (p=0.0003) in the S phase of homozygous knock-out mice, whereas the number of cells in G1 were reduced by 30% in Cdk1 $^{fl/fl}$ LysM $^{cre/cre}$ BMDMs compared to the wild type mice (p=0.0001) (Fig.10). The decrease of cells in G1 and the increase in S and G2 phase might be explained by an inability of the BMDM to go through mitosis due to the absence of a functional Cdk1.

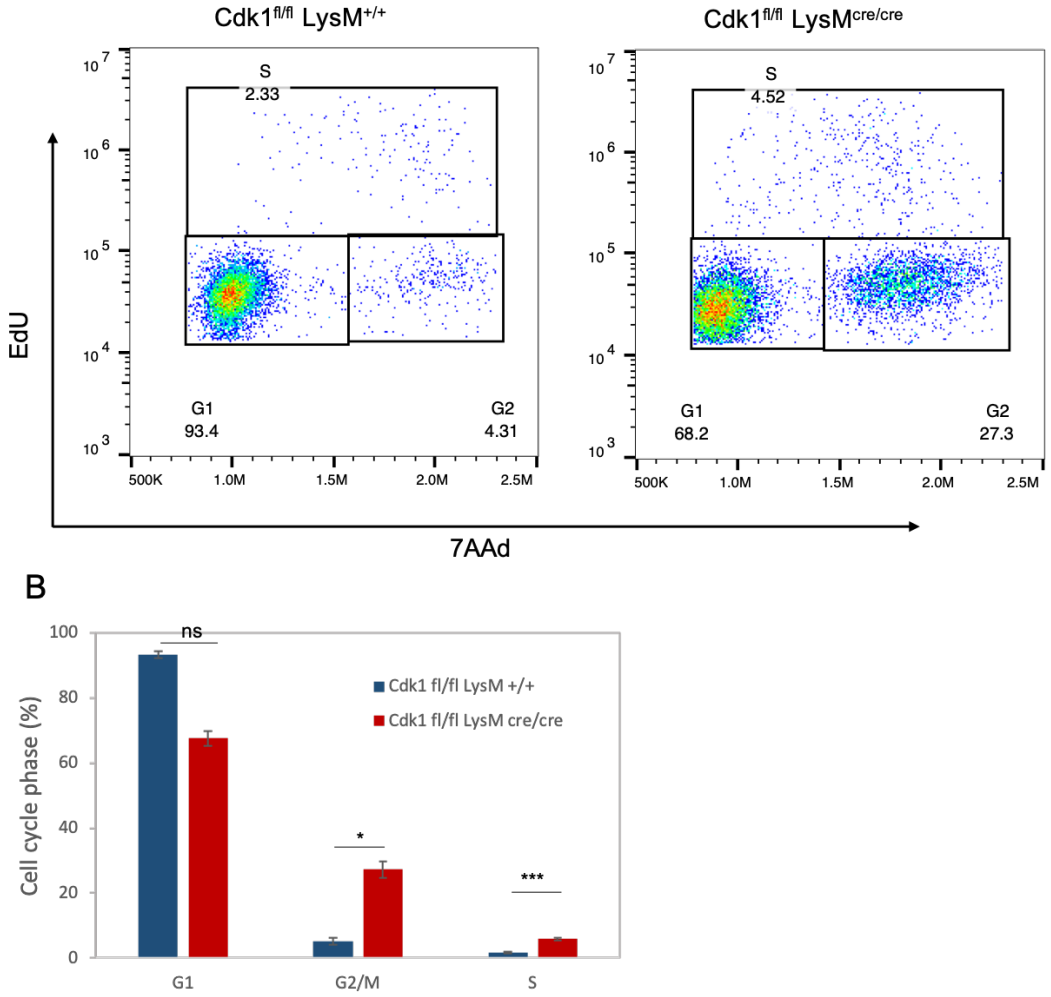

Figure 10: **Impaired cell cylce progression in Cdk1 deficient BMDM.** (**A**) Serum starved BMDMs were treated with Edu as described and analysed by flow cytometry. (**B**) The graphs represent the average frequency of cells in the cell cycle phases (n=4) with the error bar representing the SEM.

3.2.4 Cdk1 knock-out in homozygous BMDMs

To examine the amount of Cdk1 in Cdk1 $^{fl/fl}$ LysM $^{cre/cre}$ mice, we performed quantitative Real-Time PCR with the remaining BMDM (day 6). However, Cdk1 mRNA expression was only sightly, but not significantly (p= 0.3) reduced in Cdk1 $^{fl/fl}$ LysM $^{cre/cre}$ BMDMs compared to Cdk1 $^{fl/fl}$ LysM $^{+/+}$ (Fig.11A).
Although there was a slight decrease in the expression of Cdk1 protein detectable in BMDM after 6 days of differentiation (Fig.11B), it was not significant (p=0.43) (Fig.11C). Although Cdk1 should be completely absent in the homozygous Cdk1 $^{fl/fl}$ LysM $^{cre/cre}$ mice, we were still able to detect Cdk1.

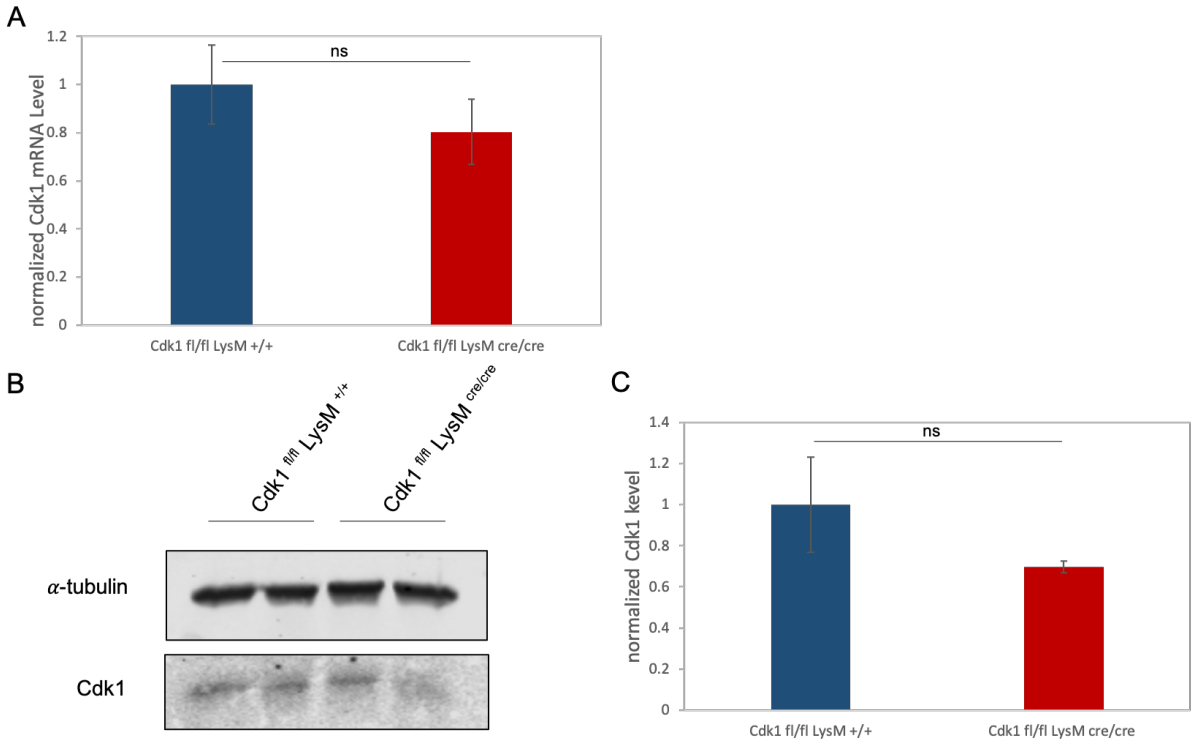

Figure 11: **Homozygous Cdk1 knock-out and expression in BMDM.** (**A**) The expression of Cdk1 mRNA in BMDM was quantified by qPCR and normalized to β-actin and Cdk1 control. (**C+B**) Samples were measured by Bradford and equal amounts loaded prior to quantification of Cdk1 protein levels by western blot. Results were normalized to α-tubulin. (**A+C**) The graphs show the average Cdk1 levels of n=2-4, with the error bar representing the SD.

3.2.5 Increased amount of RNA and Protein in Cdk1 knock-out cells

Although no significant difference in Cdk1 mRNA expression and protein synthesis was seen in the knock out and wild type cells, we noticed a 2-fold increase of total RNA (Fig.12A) and protein (Fig.12B) in the Cdk1 $^{fl/fl}$ LysM $^{cre/cre}$ BMDMs compared to Cdk1 $^{fl/fl}$ LysM $^{+/+}$. An explanation for this could be the normal progression through G1 and S phase, despite the absence of cytokinesis due to the impaired progression through mitosis. Thus, DNA is replicated and the cell grows, but no cell division takes place, therefor more total protein amount.

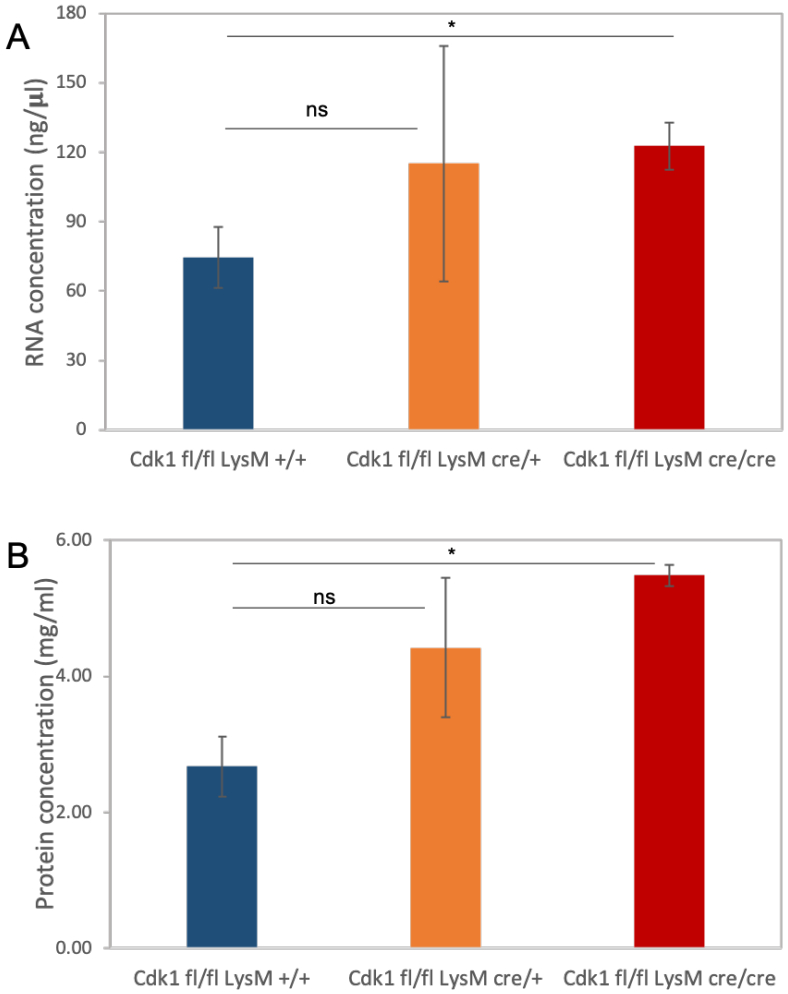

Figure 12: **Total RNA and protein levels.** (**A**) Total RNA was measured after isolation from BMDM by Nanodrop. (**B**) Total amount of protein was quantified from cell lysates by Bradford assay. (**A+B**) The graphs represent the average concentration of RNA (in ng/μl) and protein (in mg/ml) from 3-7 mice with the error bar showing the SEM.

3.3 Macrophage depletion in vivo

3.3.1 Histological staining of macrophages

We did not observe efficient deletion *in vitro*, but our data indicated that BMDM from Cdk1 $^{fl/fl}$ LysM $^{cre/+}$ mice have an impaired proliferation. Because of this, we performed immunohistochemistry with antibodies against the macrophage marker F4/80 and Tmem119, a microglial marker, to examine the reduction of macrophage numbers in vivo. We isolated various tissues and prepared them as described. The stainings were quantified using the scientific image processing program, Image J. For this reason, pictures were taken, colour channels split to separate AEC and Hematoxylen staining, and the intensity of the staining assessed (for example of quantification see Fig. 13).

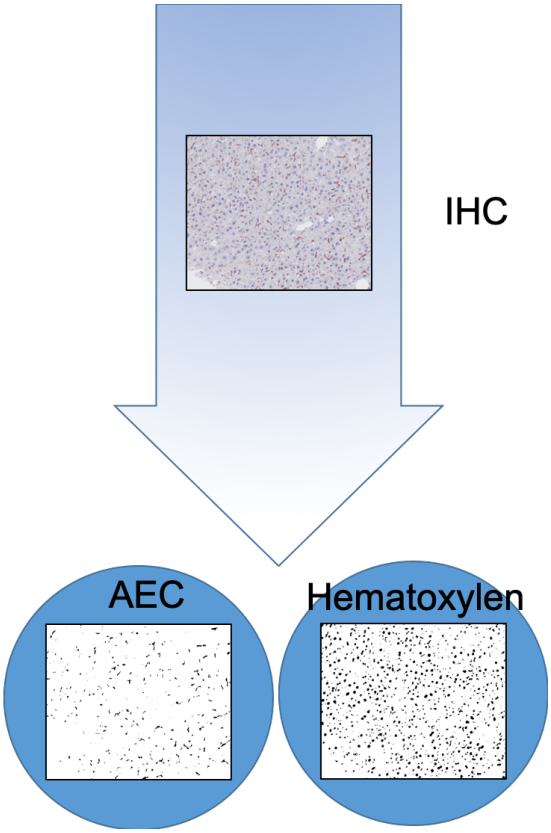

Figure 13: **Quantification of IHC by Image J.** Shown is an example of IHC quantification by Image J of hepatic tissue. For further details see text.

In the steady state, red pulp macrophages and Kupffer cells maintain themselves via a low rate of proliferation. Despite of our findings that BMDM of Cdk1 $^{fl/fl}$ LysM $^{cre/+}$ mice had a proliferative deficiency and showed reduced numbers, we detected only a slight, but not significant (p=0.57), decrease of F4/80^{+} cells in spleenic tissue (Fig.14). The same results were observed in the liver (p=0.07) (Fig.15).

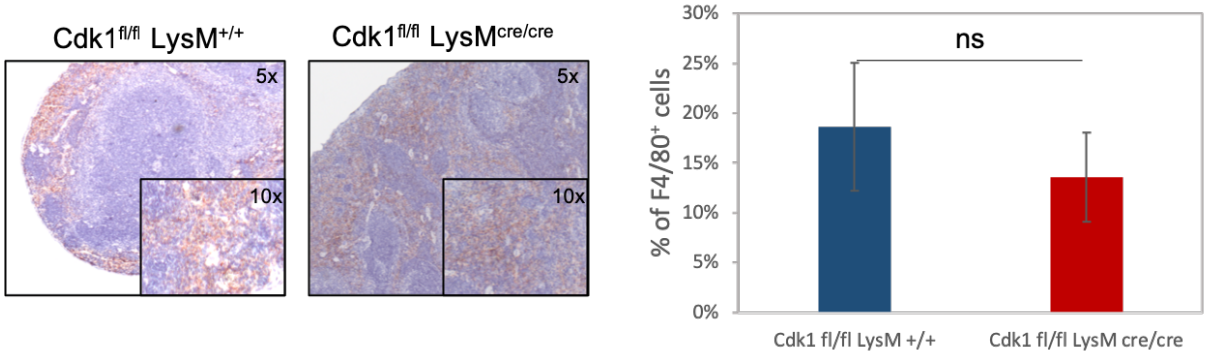

Figure 14: **F4/80 staining of spleen tissue** The number of macrophages was examined using an F4/80 antibody to stain expressing cells, quantified with Image J and normalized to cells stained with hematoxylen. The graph shows the average percentage of F4/80^{+} cells of 6 mice with the error bar representing the SEM.

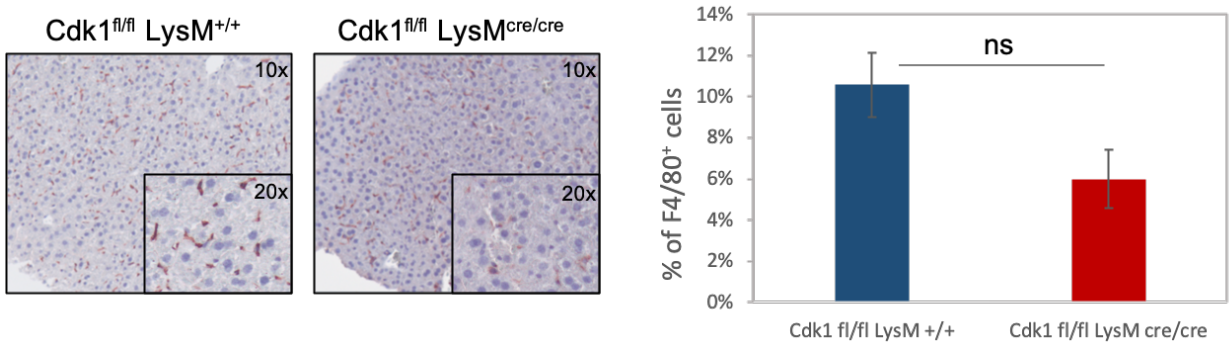

Figure 15: **F4/80 staining of liver tissue** The Number of macrophages was examined using an F4/80 antibody to stain expressing cells, quantified with Image J and normalized to cells stained with hematoxylen. The graph shows the average percentage of F4/80^{+} cells of 6 mice with the error bar representing the SEM.

Brain tissue was stained for Tmem119, a transmembrane protein specific for microglia. Due to the blood brain barrier microglia maintain their homeostasis through proliferation independent from the contribution of circulating monocytes. As expected, we saw no reduction of tissue resident macrophage numbers in the brain tissue of Cdk1 $^{fl/fl}$ LysM $^{cre/cre}$ mice compared to Cdk1 $^{fl/fl}$ LysM $^{+/+}$ mice (Fig.16), as LysM is not active in microglia, therefore Cdk1 is not deleted in microglia of Cdk1 $^{fl/fl}$ LysM $^{cre/cre}$ mice.

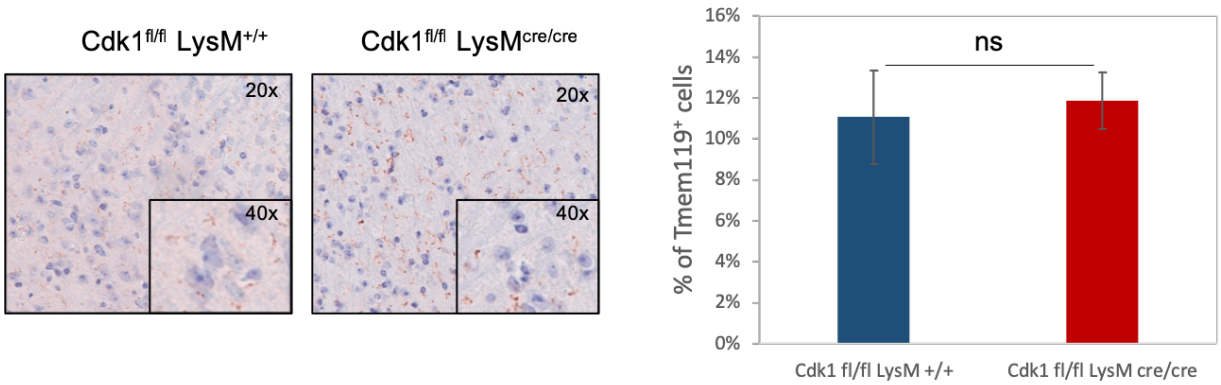

Figure 16: **Tmem119 staining of brain tissue** The number of macrophages was examined using an Tmem119 antibody to stain expressing cells, quantified with Image J and normalized to cells stained with hematoxylen. The graph shows the average percentage of $Tmem119^+$ cells of 4 mice with the error bar representing the SEM.

3.3.2 Alveolar Macrophages

Alveolar macrophages are another example of tissue resident macrophages that proliferate at a low rate and maintain themselves without almost any contribution from monocytes. However, in contrast to our findings of reduced BMDM numbers of Cdk1 $^{fl/fl}$ LysM $^{cre/cre}$ mice *in vitro*, we detected a slight, but not significant increase in lung tissues of Cdk1 $^{fl/fl}$ LysM $^{cre/cre}$ mice (p=0.37) (Fig.17). As not only alveolar macrophages show $F4/80^+$ staining, but also monocytes and interstitial macrophages, this increase might result from an influx of monocytes to compensate for the reduced number of alveolar macrophages.

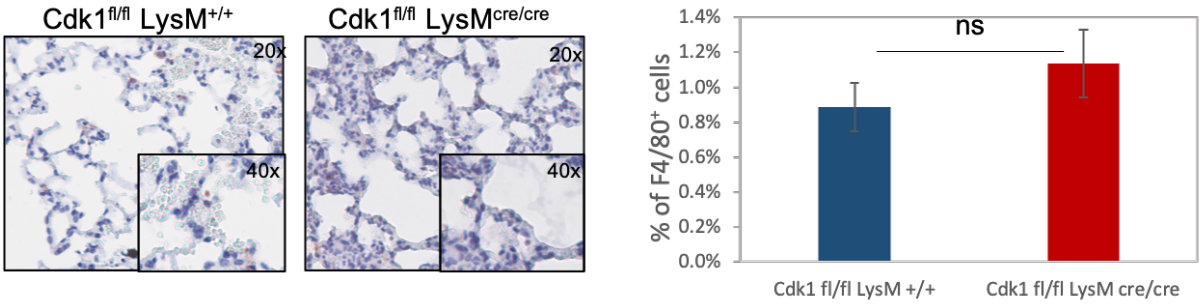

Figure 17: **F4/80 staining of lung tissue** The number of macrophages was examined using an F4/80 antibody to stain expressing cells, quantified with Image J and normalized to cells stained with hematoxylen. The graph shows the average percentage of $F4/80^+$ cells of 6 mice with the error bar representing the SEM.

Therefore, we digested murine lung lobes to isolate macrophages and stained them for flow cytometry (staining panel in the Material & Methods section). We gated for alveolar macrophages and noticed an about 2-fold decrease of $Cd11b^+SiglecF^+$ alveolar macrophages in the Cdk1 $^{fl/fl}$ LysM $^{cre/cre}$ mice compared to Cdk1 $^{fl/fl}$ LysM $^{+/+}$ (p=0.04) and Egfr $^{fl/+}$ LysM $^{cre/cre}$ (p=0.033) mice (Fig.18). This reduction in cell numbers could be due to a lack of proliferation and an impaired Cdk1 function.

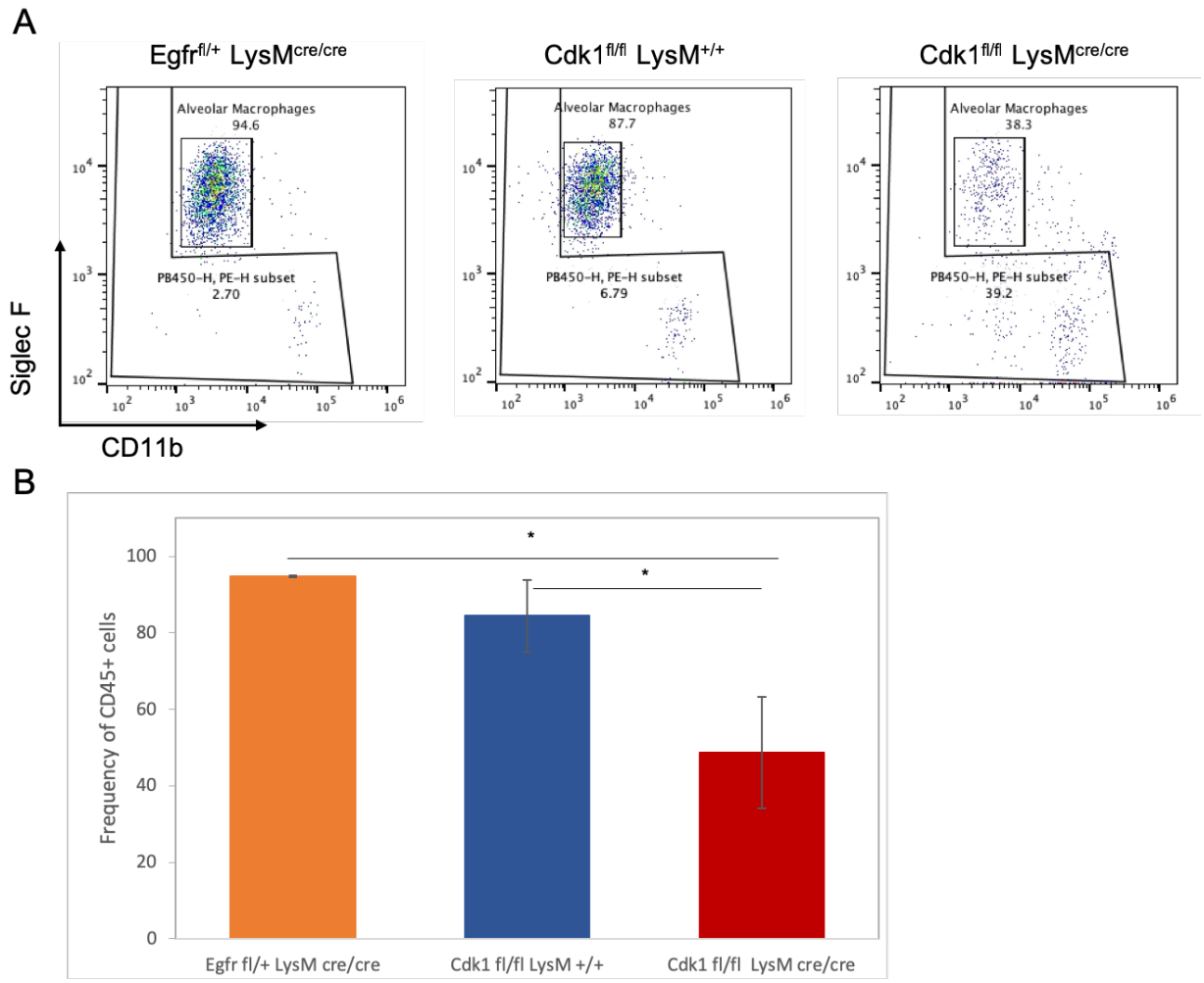

Figure 18: **Decreased alveolar macrophages in Cdk1$^{fl/fl}$ LysM$^{cre/cre}$.** (**A**) Exemplary FACS profile of alveolar macrophages. Isolation of macrophages from lung lobes was performed as described. (**B**) Quantification of $CD11b^{+}$ $SiglecF^{+}$ cells (alveolar macrophages). The graphs represent the average frequency of CD45^{+} cells (n=3-4) with the error bars representing the SD.

3.3.3 Peritoneal Macrophages

As mentioned in the introduction one subtype of peritoneal macrophages, LPMs, are able to maintain themselves by proliferation, whereas another subtype, SPMs, are argued to arise from migrating monocytes. Because of this, we also had a look at the effect of a homozygous Cdk1 knock-out on the composition of these two macrophage subtypes in the peritoneal cavity. We isolated cells from the peritoneal cavity, stained them for flow cytometry (staining panel in the Materials & Methods section) and gated for $Cd11b^{+}$ $F4/80^{+}$ cells. We were able to distinguish between large and small peritoneal macrophage (LPM and SPM) and found about 90% of LPM and 10% of SPM in both the Cdk1 $^{fl/fl}$ LysM $^{+/+}$ and Egfr $^{fl/+}$ LysM $^{cre/cre}$ controls, consistent with published literature. Interestingly, in the knock-out mice we noticed an 1.7-fold decrease of LPM (p=0.017) and a 5-fold increase of SPM (p=0.013) (Fig.19). These results suggest that LPM numbers are reduced due to a defect in proliferation. In contrast SPM are increased, possibly by the migration of monocytes to the peritoneal cavity, which are know to differentiate into SPM over time.

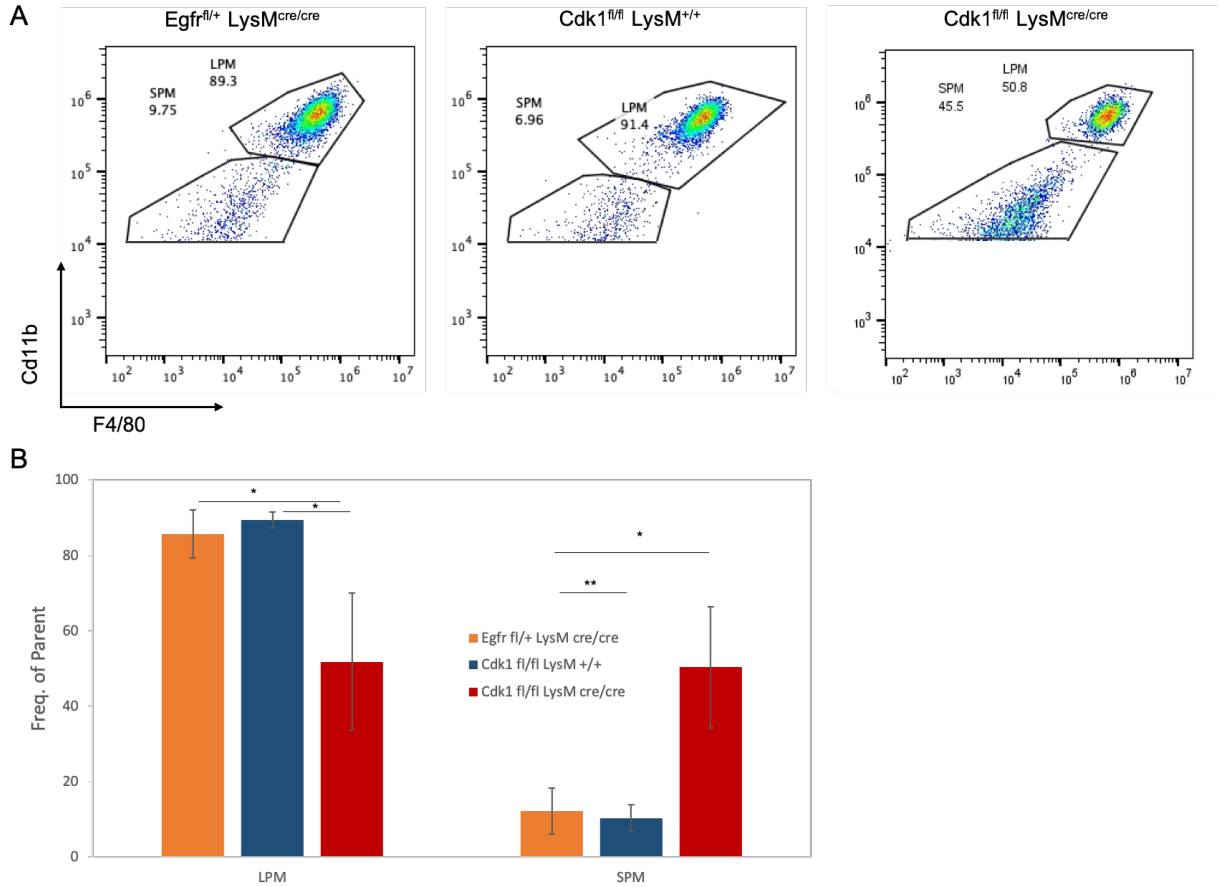

Figure 19: **Reversed profile of peritoneal macrophages in Cdk1 knock-out mice.** (**A**) Examplary FACS profile of peritoneal macrophages isolated from the peritoneal cavity as described. (**B**) Quantification of Large and Small Peritoneal Macrophages ($F4/80^{hi}$ $CD11b^{hi}$ and $F4/80^{low}$ $CD11b^{int}$) with the graphs showing the average frequency of parent (n=3-4) and the error bars representing SD.

4 Discussion

Previous studies showed, that interphase Cdks (Cdk2, Cdk4, Cdk6) are not essential for the cell cycle [71–74]. On the contrary, they can easily be compensated by the "master regulator" Cdk1. This cyclin-dependent kinase, however, cannot be compensated by other Cdks and is therefor an essential part of the cell cycle [50,77]. As a result, Cdk1$^{NULL/NULL}$ mutants are not viable [78] and only little is known about the regulation and possible additional functions of Cdk1. In order to address and overcome this problem, we used conditional knock out mice specifically targeting the ablation of Cdk1 expression in macrophages, to identify the role of Cdk1 in the cell cycle and proliferation of macrophages.

The number of Cdk1$^{fl/fl}$ LysM$^{cre/+}$ macrophages was slightly, however not significantly reduced in the BM of heterozygous Cdk1 knock-out mice. Additionally, no difference regarding mRNA expression or protein levels of Cdk1 were observed in Cdk1$^{fl/fl}$ LysM$^{cre/+}$ compared to the control. Because of these data, we hypothesised, that Cdk1 was not sufficiently knocked-out and thus generated homozygous knock-out mice.

In homozygous knock-out mice the cell number of BMDM were highly reduced compared to the control. This suggests, that differentiating cells either die due to the homozygous cre or stop proliferating. However, Egfr$^{fl/+}$ LysM$^{cre/cre}$ BMDM showed no differences in cell number compared to the Cdk1 control, therefore we excluded the possibility of the homozygous cre-allel to be cytotoxic, as was mentioned previously in the literature [80]. As the cytotoxic effect of homozygous cre- recombinase is ignorable in our mouse model, we hypothesise, that the reduction of BMDM was due to a proliferative defect. Cell cycle analysis showed more cells remaining in G2 and S phase, but in contrast less cells in the G1 phase, which indicates a proliferative defect in the progression through M phase and cytokinesis. Our results agree with the previous findings, that Cdk1 regulates the progression through and exit from mitosis.

However, mRNA expression and protein levels were not significantly reduced in this mouse model. A possible explanation for these results could be the expression and translation of Cdk1, despite the excision of exon 3. However this protein is not functional, as we were able to observe a proliferative defect. As a result, Cdk1 was still detectable in immunoblotting, because the used antibody was raised against the amino acids 224 to 230 of the Cdk1 protein (Cdc2 p34 antibody (17): sc-54, Santa Cruz Biotechnology), which are encoded in exon 4. Thus protein would still be detectable in the immunoblotting if it was translated, despite the missing exon and no function.
Another explanation for these results would be, that cells stop proliferation and undergo apoptosis after Cdk1 excision and were lost during the differentiation of BMDM. However in the remaining cells the cre recombinase did not excise Cdk1 and therefore, no change was seen at the mRNA or protein level. But still, this does not explain, why we were able to detect a proliferative defect in the remaining cells.

When looking at the total RNA and protein load of BMDMs, there was about twice as much RNA as well as protein detected in Cdk1$^{fl/fl}$ LysM$^{cre/cre}$, which suggests a cytokinesis defect in knock out mice, where cells were no longer able to divide, but

continued to grow. In those cells transcribed RNA and in succession translated protein accumulated, but was not divided to daughter cells.
Furthermore, cells of the conditional knock-out appeared to be bigger, which is also an evidence for the defective mitosis.

Since we found a defect in the progression of cells from G2 to M phase in vitro in BMDM, we wanted to confirm this proliferative defect in vivo. For this reason, histological stainings of various tissues from knock-out and wild type mice were performed.
In the splenic and hepatic tissue of conditional knock-out mice reduced numbers of $F4/80^+$ macrophages were detected, but these results were not significant. Red pulp macrophages and Kupffer cells have a long lifespan, but a low rate of proliferation during steady conditions [81, 82]. Challenging $Cdk1^{fl/fl}$ $LysM^{cre/cre}$ mice with non-genotoxic ablation of tissue resident macrophages with e.g. a parasitic infection might induce proliferation in those cells and give us a better idea of the importance of Cdk1 in macrophages.
In brain tissue no change in $F4/80^+$ expression levels were noticed. However it is known that no LysM activity is detectable in the brain [83], therefore no excision of exon 3 in the Cdk1 locus occurs and thus explains the missing reduction of macrophage numbers in $Cdk1^{fl/fl}$ $LysM^{cre/cre}$ mice. Usage of a different mouse model with the cre recombinase under a different promotor, for example CX3CR1, which is also expressed in microglia, would overcome this obstacle and elucidate the role of Cdk1 in microglial proliferation.

In contrast to the slightly reduced macrophage numbers in hepatic and splenic tissue, we noticed increased values of $F4/80^+$ cells in the lung tissue of $Cdk1^{fl/fl}$ $LysM^{cre/cre}$ mice. These results were contrary to our expectations. Nevertheless, positive F4/80-staining is not only a marker of alveolar, but also interstitial macrophages and even monocytes [84]. In flow cytometric analysis of lung tissue we were better able to distinguish between alveolar macrophages and other cell types in the lung lobes of Cdk1 deficient mice and detected a reduction of $Cd11b^+$ $SiglecF^+$ cells (alveolar macrophages).

The analysis of peritoneal macrophages showed a phenotype similar to that of an inflammatory state of the peritoneal cavity in $Cdk1^{fl/fl}LysM^{cre/cre}$ mice, where large peritoneal macrophages were reduced and small peritoneal macrophages increased. In contrast, wild type mice ($Cdk1^{fl/fl}LysM^{+/+}$) depicted the phenotype of healthy mice under steady state conditions [40, 43, 45]. We hypothesise the increased influx of monocytes and the resulting massive arise of SPM to compensate for reduction of LPM due to the reduced proliferative capacity.

In a cell, one of the most important objectives is proliferation and mitosis These are strongly regulated processes, requiring many different proteins to progress through the cell cycle. The cyclin-dependent kinase 1 (Cdk1) is part of this regulatory machinery and is able to compensate for absent interphase Cdks without any detectable defects. However, no other protein kinase is able to compensate for the loss of Cdk1, therefore makes it an essential cyclin-dependent kinase for the cell cycle.
Throughout the years, studies with conditional knock-outs of Cdk1 have been performed in different cell types. For instance, a knock-out of Cdk1 in oocytes led to infertility due to a meiotic arrest at the germinal vesicle stage [85].

In another study, Cdk1 knock-out in hepatocytes led to an absence of cell division in adult hepatocytes after partial hepatectomy [78]. However, complete regeneration was achieved in the knock-out mice by cell growth rather than cell division.
Our findings show that Cdk1 depletion in macrophages and neutrophils reduces macrophage numbers in vivo in alveolar and large peritoneal macrophages. Additionally, we detected an increase in small peritoneal macrophages to compensate for the loss of LPMs.
As Cdk1 controls, among others, the entry into mitosis, chromosome condensation, breakdown of nuclear lamins and the disassembly of the Golgi apparatus [66–68], its absence in macrophages results in a blockage of the cell cycle at the G2-phase. Subsequent to the prolonged S-phase and the resulting accumulation of re-replicated DNA, RNA and protein, bone marrow derived macrophages not only showed an increase in size in vitro, but were also reduced in numbers, due to the defective proliferation.

In this work we proposed the reduction in macrophage numbers to be due to a proliferative defect in the transition of the G2 to M phase. However, we only showed this in vitro in bone marrow derived macrophages. Therefore, a proliferation assay of tissue resident macrophages, such as alveolar macrophages or peritoneal macrophages has to be performed in the future, to confirm the correlation between Cdk1 depletion, impaired proliferation and reduced macrophage numbers in vivo.
Secondly, since we were not able to determine the efficiency of the recombination by qPCR or Western Blot, a different strategy has to be developed. As it might be possible, that differentiating bone marrow-derived macrophages might stop proliferation and undergo apoptosis after recombination, we should harvest the dead cells in the supernatant, purify for F4/80$^+$ cells and check recombination frequency in the obtained cells. Furthermore, recombination should be detected in isolated tissue macrophages, for example alveolar macrophages or peritoneal macrophages.
Additionally, using a different mouse model, e.g. conditional knock-out of CX3CR1, for the analysis of tissue resident macrophages might show an effect in microglia, as Lysozym M is not active in brain tissue.

Finally, tissue macrophages and myeloid progenitors in the BM proliferate to maintain homeostasis and to recover the macrophage pool after an injury or infection.
However, excessive proliferation of macrophages can have damaging properties. For instance, accumulation of macrophages in adipose tissue during obesity leads to chronic inflammation, which in turn leads to metabolic disorders, such as diabetes [86]. Similarly, local proliferation and accumulation of lesional macrophages in atherosclerotic plaques also produce inflammatory mediators, which exacerbate the disease [87]. Further, inhibition of progressive expansion of microglia decreased the number of degenerating neurons and had beneficial effects over the progression of chronic neurodegeneration [88]. Likewise, the depletion of tumour-associated macrophages from the tumour microenviroment blocked their pro-tumoral function [89].
In contrast, in the model of experimental autoimmune encephalomyelitis (EAE), an animal model of multiple sclerosis, monocyte-derived macrophages appear to initiate demyelination, whereas microglia seem inert at disease onset. Re-stimulation of the proliferative capacity of microglia therefore might prevent the influx of inflammatory monocytes and improves the outcome of the disease [90].

A better understanding of the precise role of Cdk1 in the proliferation of macrophages and the contribution of local proliferation in inflammatory and non-inflammatory conditions might further be relevant for the treatment of disease, where enhanced macrophage proliferation is either beneficial or disadvantageous for the outcome of the disease.

5 References

[1] Elias Metschnikoff. Ueber eine sprosspilzkrankheit der daphnien. beitrag zur lehre über den kampf der phagocyten gegen krankheitserreger. *Archiv für Pathologische Anatomie und Physiologie und für Klinische Medicin*, 96(2):177–195, may 1884.

[2] Darin K Fogg, Claire Sibon, Chaouki Miled, Steffen Jung, Pierre Aucouturier, Dan R Littman, Ana Cumano, and Frederic Geissmann. A clonogenic bone marrow progenitor specific for macrophages and dendritic cells. *Science*, 311(5757):83–87, jan 2006.

[3] R van Furth and Z A Cohn. The origin and kinetics of mononuclear phagocytes. *The Journal of Experimental Medicine*, 128(3):415–435, sep 1968.

[4] Florent Ginhoux, Melanie Greter, Marylene Leboeuf, Sayan Nandi, Peter See, Solen Gokhan, Mark F Mehler, Simon J Conway, Lai Guan Ng, E Richard Stanley, Igor M Samokhvalov, and Miriam Merad. Fate mapping analysis reveals that adult microglia derive from primitive macrophages. *Science*, 330(6005):841–845, nov 2010.

[5] Daigo Hashimoto, Andrew Chow, Clara Noizat, Pearline Teo, Mary Beth Beasley, Marylene Leboeuf, Christian D Becker, Peter See, Jeremy Price, Daniel Lucas, Melanie Greter, Arthur Mortha, Scott W Boyer, E Camilla Forsberg, Masato Tanaka, Nico van Rooijen, Adolfo García-Sastre, E Richard Stanley, Florent Ginhoux, Paul S Frenette, and Miriam Merad. Tissue-resident macrophages self-maintain locally throughout adult life with minimal contribution from circulating monocytes. *Immunity*, 38(4):792–804, apr 2013.

[6] Bahareh Ajami, Jami L Bennett, Charles Krieger, Kelly M McNagny, and Fabio M V Rossi. Infiltrating monocytes trigger EAE progression, but do not contribute to the resident microglia pool. *Nature Neuroscience*, 14(9):1142–1149, jul 2011.

[7] Thomas A Wynn, Ajay Chawla, and Jeffrey W Pollard. Macrophage biology in development, homeostasis and disease. *Nature*, 496(7446):445–455, apr 2013.

[8] Stuart H Orkin and Leonard I Zon. Hematopoiesis: an evolving paradigm for stem cell biology. *Cell*, 132(4):631–644, feb 2008.

[9] A M Lichanska and D A Hume. Origins and functions of phagocytes in the embryo. *Experimental Hematology*, 28(6):601–611, jun 2000.

[10] A M Müller, A Medvinsky, J Strouboulis, F Grosveld, and E Dzierzak. Development of hematopoietic stem cell activity in the mouse embryo. *Immunity*, 1(4):291–301, jul 1994.

[11] Ana Cumano and Isabelle Godin. Ontogeny of the hematopoietic system. *Annual Review of Immunology*, 25:745–785, 2007.

[12] Julien Y Bertrand, Abdelali Jalil, Michèle Klaine, Steffen Jung, Ana Cumano, and Isabelle Godin. Three pathways to mature macrophages in the early mouse yolk sac. *Blood*, 106(9):3004–3011, nov 2005.

[13] Igor M Samokhvalov, Natalia I Samokhvalova, and Shin-ichi Nishikawa. Cell tracing shows the contribution of the yolk sac to adult haematopoiesis. *Nature*, 446(7139):1056–1061, apr 2007.

[14] Christian Schulz, Elisa Gomez Perdiguero, Laurent Chorro, Heather Szabo-Rogers, Nicolas Cagnard, Katrin Kierdorf, Marco Prinz, Bishan Wu, Sten Eirik W Jacobsen, Jeffrey W Pollard, Jon Frampton, Karen J Liu, and Frederic Geissmann. A lineage of myeloid cells independent of myb and hematopoietic stem cells. *Science*, 336(6077):86–90, apr 2012.

[15] Kaaweh Molawi, Yochai Wolf, Prashanth K Kandalla, Jeremy Favret, Nora Hagemeyer, Kathrin Frenzel, Alexander R Pinto, Kay Klapproth, Sandrine Henri, Bernard Malissen, Hans-Reimer Rodewald, Nadia A Rosenthal, Marc Bajenoff, Marco Prinz, Steffen Jung, and Michael H Sieweke. Progressive replacement of embryo-derived cardiac macrophages with age. *The Journal of Experimental Medicine*, 211(11):2151–2158, oct 2014.

[16] Monica R P Elmore, Allison R Najafi, Maya A Koike, Nabil N Dagher, Elizabeth E Spangenberg, Rachel A Rice, Masashi Kitazawa, Bernice Matusow, Hoa Nguyen, Brian L West, and Kim N Green. Colony-stimulating factor 1 receptor signaling is necessary for microglia viability, unmasking a microglia progenitor cell in the adult brain. *Neuron*, 82(2):380–397, apr 2014.

[17] Clément Ghigo, Isabelle Mondor, Audrey Jorquera, Jonathan Nowak, Stephan Wienert, Sonja P Zahner, Björn E Clausen, Hervé Luche, Bernard Malissen, Frederick Klauschen, and Marc Bajénoff. Multicolor fate mapping of langerhans cell homeostasis. *The Journal of Experimental Medicine*, 210(9):1657–1664, aug 2013.

[18] Y Shibata, P Y Berclaz, Z C Chroneos, M Yoshida, J A Whitsett, and B C Trapnell. GM-CSF regulates alveolar macrophage differentiation and innate immunity in the lung through PU.1. *Immunity*, 15(4):557–567, oct 2001.

[19] Fernando O Martinez, Laura Helming, Ronny Milde, Audrey Varin, Barbro N Melgert, Christina Draijer, Benjamin Thomas, Marco Fabbri, Anjali Crawshaw, Ling Pei Ho, Nick H Ten Hacken, Viviana Cobos Jiménez, Neeltje A Kootstra, Jörg Hamann, David R Greaves, Massimo Locati, Alberto Mantovani, and Siamon Gordon. Genetic programs expressed in resting and IL-4 alternatively activated mouse and human macrophages: similarities and differences. *Blood*, 121(9):e57–69, feb 2013.

[20] M Stein, S Keshav, N Harris, and S Gordon. Interleukin 4 potently enhances murine macrophage mannose receptor activity: a marker of alternative immunologic macrophage activation. *The Journal of Experimental Medicine*, 176(1):287–292, jul 1992.

[21] Stephen J Jenkins, Dominik Ruckerl, Graham D Thomas, James P Hewitson, Sheelagh Duncan, Frank Brombacher, Rick M Maizels, David A Hume, and Judith E Allen. IL-4 directly signals tissue-resident macrophages to proliferate beyond homeostatic levels controlled by CSF-1. *The Journal of Experimental Medicine*, 210(11):2477–2491, oct 2013.

[22] Joshua D Milner, Tatyana Orekov, Jerrold M Ward, Lily Cheng, Fernando Torres-Velez, Ilkka Junttila, Guangping Sun, Mark Buller, Suzanne C Morris, Fred D Finkelman, and William E Paul. Sustained IL-4 exposure leads to a novel pathway for hemophagocytosis, inflammation, and tissue macrophage accumulation. *Blood*, 116(14):2476–2483, oct 2010.

[23] Dominik Rückerl, Stephen J Jenkins, Nouf N Laqtom, Iain J Gallagher, Tara E Sutherland, Sheelagh Duncan, Amy H Buck, and Judith E Allen. Induction of il-4ralpha-dependent microrna identifies pi3k/akt signaling as essential for il-4-driven murine macrophage proliferation in vivo. *Blood*, 120(11):2307–2316, sep 2012.

[24] Luke C Davies, Marcela Rosas, Stephen J Jenkins, Chia-Te Liao, Martin J Scurr, Frank Brombacher, Donald J Fraser, Judith E Allen, Simon A Jones, and Philip R Taylor. Distinct bone marrow-derived and tissue-resident macrophage lineages proliferate at key stages during inflammation. *Nature Communications*, 4:1886, 2013.

[25] W W Wiktor-Jedrzejczak, A Ahmed, C Szczylik, and R R Skelly. Hematological characterization of congenital osteopetrosis in op/op mouse. possible mechanism for abnormal macrophage differentiation. *The Journal of Experimental Medicine*, 156(5):1516–1527, nov 1982.

[26] Florent Ginhoux, Frank Tacke, Veronique Angeli, Milena Bogunovic, Martine Loubeau, Xu-Ming Dai, E Richard Stanley, Gwendalyn J Randolph, and Miriam Merad. Langerhans cells arise from monocytes in vivo. *Nature Immunology*, 7(3):265–273, mar 2006.

[27] Valerie Garceau, Jacqueline Smith, Ian R Paton, Megan Davey, Mario A Fares, David P Sester, David W Burt, and David A Hume. Pivotal advance: Avian colony-stimulating factor 1 (CSF-1), interleukin-34 (IL-34), and CSF-1 receptor genes and gene products. *Journal of Leukocyte Biology*, 87(5):753–764, may 2010.

[28] Haishan Lin, Ernestine Lee, Kevin Hestir, Cindy Leo, Minmei Huang, Elizabeth Bosch, Robert Halenbeck, Ge Wu, Aileen Zhou, Dirk Behrens, Diane Hollenbaugh, Thomas Linnemann, Minmin Qin, Justin Wong, Keting Chu, Stephen K Doberstein, and Lewis T Williams. Discovery of a cytokine and its receptor by functional screening of the extracellular proteome. *Science*, 320(5877):807–811, may 2008.

[29] Melanie Greter, Iva Lelios, Pawel Pelczar, Guillaume Hoeffel, Jeremy Price, Marylene Leboeuf, Thomas M Kündig, Karl Frei, Florent Ginhoux, Miriam Merad, and Burkhard Becher. Stroma-derived interleukin-34 controls the development and maintenance of langerhans cells and the maintenance of microglia. *Immunity*, 37(6):1050–1060, dec 2012.

[30] T Chihara, S Suzu, R Hassan, N Chutiwitoonchai, M Hiyoshi, K Motoyoshi, F Kimura, and S Okada. IL-34 and m-CSF share the receptor fms but are not identical in biological activity and signal activation. *Cell Death and Differentiation*, 17(12):1917–1927, dec 2010.

[31] D M Bortner, M Ulivi, M F Roussel, and M C Ostrowski. The carboxy-terminal catalytic domain of the GTPase-activating protein inhibits nuclear signal transduction and morphological transformation mediated by the CSF-1 receptor. *Genes & Development*, 5(10):1777–1785, oct 1991.

[32] S J Langer, D M Bortner, M F Roussel, C J Sherr, and M C Ostrowski. Mitogenic signaling by colony-stimulating factor 1 and ras is suppressed by the ets-2 DNA-binding domain and restored by myc overexpression. *Molecular and Cellular Biology*, 12(12):5355–5362, dec 1992.

[33] M A Reddy, S J Langer, M S Colman, and M C Ostrowski. An enhancer element responsive to ras and fms signaling pathways is composed of two distinct nuclear factor binding sites. *Molecular Endocrinology*, 6(7):1051–1060, jul 1992.

[34] Rebecca Gentek, Kaaweh Molawi, and Michael H Sieweke. Tissue macrophage identity and self-renewal. *Immunological Reviews*, 262(1):56–73, nov 2014.

[35] S P Hedge, A Kumar, C Kurschner, and L H Shapiro. c-maf interacts with c-myb to regulate transcription of an early myeloid gene during differentiation. *Molecular and Cellular Biology*, 18(5):2729–2737, may 1998.

[36] Silke Tillmanns, Claas Otto, Ellis Jaffray, Camille Du Roure, Youssef Bakri, Laurent Vanhille, Sandrine Sarrazin, Ronald T Hay, and Michael H Sieweke. SUMO modification regulates MafB-driven macrophage differentiation by enabling myb-dependent transcriptional repression. *Molecular and Cellular Biology*, 27(15):5554–5564, aug 2007.

[37] M H Sieweke, H Tekotte, J Frampton, and T Graf. MafB is an interaction partner and repressor of ets-1 that inhibits erythroid differentiation. *Cell*, 85(1):49–60, apr 1996.

[38] Monika Linke, Ha Thi Thanh Pham, Karl Katholnig, Thomas Schnöller, Anne Miller, Florian Demel, Birgit Schütz, Margit Rosner, Boris Kovacic, Nyamdelger Sukhbaatar, Birgit Niederreiter, Stephan Blüml, Peter Kuess, Veronika Sexl, Mathias Müller, Mario Mikula, Wolfram Weckwerth, Arvand Haschemi, Martin Susani, Markus Hengstschläger, Michael J Gambello, and Thomas Weichhart. Chronic signaling via the metabolic checkpoint kinase mTORC1 induces macrophage granuloma formation and marks sarcoidosis progression. *Nature Immunology*, 18(3):293–302, jan 2017.

[39] Hui-Ju Hsieh, Wei Zhang, Shu-Hong Lin, Wen-Hao Yang, Jun-Zhong Wang, Jianfeng Shen, Yiran Zhang, Yiling Lu, Hua Wang, Jane Yu, Gordon B Mills, and Guang Peng. Systems biology approach reveals a link between mTORC1 and g2/m DNA damage checkpoint recovery. *Nature Communications*, 9(1):3982, sep 2018.

[40] Eliver Eid Bou Ghosn, Alexandra A Cassado, Gregory R Govoni, Takeshi Fukuhara, Yang Yang, Denise M Monack, Karina R Bortoluci, Sandro R Almeida, Leonard A Herzenberg, and Leonore A Herzenberg. Two physically, functionally, and developmentally distinct peritoneal macrophage subsets. *Proceedings of the National Academy of Sciences of the United States of America*, 107(6):2568–2573, feb 2010.

[41] Vincent Dioszeghy, Marcela Rosas, Benjamin H Maskrey, Chantal Colmont, Nicholas Topley, Pavlos Chaitidis, Hartmut Kühn, Simon A Jones, Philip R Taylor, and Valerie B O'Donnell. 12/15-lipoxygenase regulates the inflammatory response to bacterial products in vivo. *Journal of Immunology*, 181(9):6514–6524, nov 2008.

[42] Siamon Gordon and Philip R Taylor. Monocyte and macrophage heterogeneity. *Nature Reviews. Immunology*, 5(12):953–964, dec 2005.

[43] Derek W Cain, Emily G O'Koren, Matthew J Kan, Mandy Womble, Gregory D Sempowski, Kristen Hopper, Michael D Gunn, and Garnett Kelsoe. Identification of a tissue-specific, c/ebp beta-dependent pathway of differentiation for murine peritoneal macrophages. *Journal of Immunology*, 191(9):4665–4675, nov 2013.

[44] M J Melnicoff, P K Horan, E W Breslin, and P S Morahan. Maintenance of peritoneal macrophages in the steady state. *Journal of Leukocyte Biology*, 44(5):367–375, nov 1988.

[45] Luke C Davies, Marcela Rosas, Paul J Smith, Donald J Fraser, Simon A Jones, and Philip R Taylor. A quantifiable proliferative burst of tissue macrophages restores homeostatic macrophage populations after acute inflammation. *European Journal of Immunology*, 41(8):2155–2164, aug 2011.

[46] Jing Wang and Paul Kubes. A reservoir of mature cavity macrophages that can rapidly invade visceral organs to affect tissue repair. *Cell*, 165(3):668–678, apr 2016.

[47] M W Barth, J A Hendrzak, M J Melnicoff, and P S Morahan. Review of the macrophage disappearance reaction. *Journal of Leukocyte Biology*, 57(3):361–367, mar 1995.

[48] N Jonjić, G Peri, S Bernasconi, F L Sciacca, F Colotta, P Pelicci, L Lanfrancone, and A Mantovani. Expression of adhesion molecules and chemotactic cytokines in cultured human mesothelial cells. *The Journal of Experimental Medicine*, 176(4):1165–1174, oct 1992.

[49] Yasutaka Okabe and Ruslan Medzhitov. Tissue-specific signals control reversible program of localization and functional polarization of macrophages. *Cell*, 157(4):832–844, may 2014.

[50] A Satyanarayana and P Kaldis. Mammalian cell-cycle regulation: several cdks, numerous cyclins and diverse compensatory mechanisms. *Oncogene*, 28(33):2925–2939, aug 2009.

[51] Marcos Malumbres. Cyclin-dependent kinases. *Genome Biology*, 15(6):122, 2014.

[52] P Russell and P Nurse. Schizosaccharomyces pombe and saccharomyces cerevisiae: a look at yeasts divided. *Cell*, 45(6):781–782, jun 1986.

[53] G Draetta, L Brizuela, J Potashkin, and D Beach. Identification of p34 and p13, human homologs of the cell cycle regulators of fission yeast encoded by cdc2+ and suc1+. *Cell*, 50(2):319–325, jul 1987.

[54] Lihuan Cao, Fang Chen, Xianmei Yang, Weijin Xu, Jun Xie, and Long Yu. Phylogenetic analysis of CDK and cyclin proteins in premetazoan lineages. *BMC Evolutionary Biology*, 14:10, jan 2014.

[55] John H Doonan and Georgios Kitsios. Functional evolution of cyclin-dependent kinases. *Molecular Biotechnology*, 42(1):14–29, may 2009.

[56] Marcos Malumbres and Mariano Barbacid. Mammalian cyclin-dependent kinases. *Trends in Biochemical Sciences*, 30(11):630–641, nov 2005.

[57] M Malumbres and M Barbacid. To cycle or not to cycle: a critical decision in cancer. *Nature Reviews. Cancer*, 1(3):222–231, dec 2001.

[58] C J Sherr and J M Roberts. CDK inhibitors: positive and negative regulators of g1-phase progression. *Genes & Development*, 13(12):1501–1512, jun 1999.

[59] J H Dannenberg, A van Rossum, L Schuijff, and H te Riele. Ablation of the retinoblastoma gene family deregulates g(1) control causing immortalization and increased cell turnover under growth-restricting conditions. *Genes & Development*, 14(23):3051–3064, dec 2000.

[60] M Ohtsubo, A M Theodoras, J Schumacher, J M Roberts, and M Pagano. Human cyclin e, a nuclear protein essential for the g1-to-s phase transition. *Molecular and Cellular Biology*, 15(5):2612–2624, may 1995.

[61] D M Koepp, L K Schaefer, X Ye, K Keyomarsi, C Chu, J W Harper, and S J Elledge. Phosphorylation-dependent ubiquitination of cyclin e by the SCFFbw7 ubiquitin ligase. *Science*, 294(5540):173–177, oct 2001.

[62] Alex C Minella, Jherek Swanger, Eileen Bryant, Markus Welcker, Harry Hwang, and Bruce E Clurman. p53 and p21 form an inducible barrier that protects cells against cyclin e-cdk2 deregulation. *Current Biology*, 12(21):1817–1827, oct 2002.

[63] D Coverley, C Pelizon, S Trewick, and R A Laskey. Chromatin-bound cdc6 persists in s and g2 phases in human cells, while soluble cdc6 is destroyed in a cyclin a-cdk2 dependent process. *Journal of Cell Science*, 113 (Pt 11):1929–1938, jun 2000.

[64] B O Petersen, J Lukas, C S Sorensen, J Bartek, and K Helin. Phosphorylation of mammalian cdc6 by cyclin a/cdk2 regulates its subcellular localization. *The EMBO Journal*, 18(2):396–410, jan 1999.

[65] M M Koseoglu, L M Graves, and W F Marzluff. Phosphorylation of threonine 61 by cyclin a/cdk1 triggers degradation of stem-loop binding protein at the end of s phase. *Molecular and Cellular Biology*, 28(14):4469–4479, jul 2008.

[66] M Lowe, C Rabouille, N Nakamura, R Watson, M Jackman, E Jämsä, D Rahman, D J Pappin, and G Warren. Cdc2 kinase directly phosphorylates the cis-golgi matrix protein GM130 and is required for golgi fragmentation in mitosis. *Cell*, 94(6):783–793, sep 1998.

[67] Christian Preisinger, Roman Körner, Mathias Wind, Wolf D Lehmann, Robert Kopajtich, and Francis A Barr. Plk1 docking to GRASP65 phosphorylated by cdk1 suggests a mechanism for golgi checkpoint signalling. *The EMBO Journal*, 24(4):753–765, feb 2005.

[68] M Peter, J Nakagawa, M Dorée, J C Labbé, and E A Nigg. In vitro disassembly of the nuclear lamina and m phase-specific phosphorylation of lamins by cdc2 kinase. *Cell*, 61(4):591–602, may 1990.

[69] M A Félix, J C Labbé, M Dorée, T Hunt, and E Karsenti. Triggering of cyclin degradation in interphase extracts of amphibian eggs by cdc2 kinase. *Nature*, 346(6282):379–382, jul 1990.

[70] A W Murray, M J Solomon, and M W Kirschner. The role of cyclin synthesis and degradation in the control of maturation promoting factor activity. *Nature*, 339(6222):280–286, may 1989.

[71] Cyril Berthet, Eiman Aleem, Vincenzo Coppola, Lino Tessarollo, and Philipp Kaldis. Cdk2 knockout mice are viable. *Current Biology*, 13(20):1775–1785, oct 2003.

[72] Sagrario Ortega, Ignacio Prieto, Junko Odajima, Alberto Martín, Pierre Dubus, Rocio Sotillo, Jose Luis Barbero, Marcos Malumbres, and Mariano Barbacid. Cyclin-dependent kinase 2 is essential for meiosis but not for mitotic cell division in mice. *Nature Genetics*, 35(1):25–31, sep 2003.

[73] S G Rane, P Dubus, R V Mettus, E J Galbreath, G Boden, E P Reddy, and M Barbacid. Loss of cdk4 expression causes insulin-deficient diabetes and cdk4 activation results in beta-islet cell hyperplasia. *Nature Genetics*, 22(1):44–52, may 1999.

[74] Miaofen G Hu, Amit Deshpande, Miriam Enos, Daqin Mao, Elisabeth A Hinds, Guo-fu Hu, Rui Chang, Zhuyan Guo, Marei Dose, Changchuin Mao, Philip N Tsichlis, Fotini Gounari, and Philip W Hinds. A requirement for cyclin-dependent kinase 6 in thymocyte development and tumorigenesis. *Cancer Research*, 69(3):810–818, feb 2009.

[75] Marcos Malumbres, Rocío Sotillo, David Santamaría, Javier Galán, Ana Cerezo, Sagrario Ortega, Pierre Dubus, and Mariano Barbacid. Mammalian cells cycle without the d-type cyclin-dependent kinases cdk4 and cdk6. *Cell*, 118(4):493–504, aug 2004.

[76] Cyril Berthet, Kimberly D Klarmann, Mary Beth Hilton, Hyung Chan Suh, Jonathan R Keller, Hiroaki Kiyokawa, and Philipp Kaldis. Combined loss of cdk2 and cdk4 results in embryonic lethality and rb hypophosphorylation. *Developmental Cell*, 10(5):563–573, may 2006.

[77] Ande Satyanarayana, Cyril Berthet, Javier Lopez-Molina, Vincenzo Coppola, Lino Tessarollo, and Philipp Kaldis. Genetic substitution of cdk1 by cdk2 leads to embryonic lethality and loss of meiotic function of cdk2. *Development*, 135(20):3389–3400, oct 2008.

[78] M Kasim Diril, Chandrahas Koumar Ratnacaram, V C Padmakumar, Tiehua Du, Martin Wasser, Vincenzo Coppola, Lino Tessarollo, and Philipp Kaldis. Cyclin-dependent kinase 1 (cdk1) is essential for cell division and suppression of DNA re-replication but not for liver regeneration. *Proceedings of the National Academy of Sciences of the United States of America*, 109(10):3826–3831, mar 2012.

[79] B.E. Clausen, C. Burkhardt, W. Reith, R. Renkawitz, and I. Förster. Conditional gene targeting in macrophages and granulocytes using LysMcre mice. *Transgenic Research*, 8(4):265–277, aug 1999.

[80] A Loonstra, M Vooijs, H B Beverloo, B A Allak, E van Drunen, R Kanaar, A Berns, and J Jonkers. Growth inhibition and DNA damage induced by cre recombinase in mammalian cells. *Proceedings of the National Academy of Sciences of the United States of America*, 98(16):9209–9214, jul 2001.

[81] Daisuke Kurotaki, Toshimitsu Uede, and Tomohiko Tamura. Functions and development of red pulp macrophages. *Microbiology and Immunology*, 59(2):55–62, feb 2015.

[82] Simon Yona, Ki-Wook Kim, Yochai Wolf, Alexander Mildner, Diana Varol, Michal Breker, Dalit Strauss-Ayali, Sergey Viukov, Martin Guilliams, Alexander Misharin, David A Hume, Harris Perlman, Bernard Malissen, Elazar Zelzer, and Steffen Jung. Fate mapping reveals origins and dynamics of monocytes and tissue macrophages under homeostasis. *Immunity*, 38(1):79–91, jan 2013.

[83] M Cross, I Mangelsdorf, A Wedel, and R Renkawitz. Mouse lysozyme m gene: isolation, characterization, and expression studies. *Proceedings of the National Academy of Sciences of the United States of America*, 85(17):6232–6236, sep 1988.

[84] Rinat Zaynagetdinov, Taylor P Sherrill, Peggy L Kendall, Brahm H Segal, Kevin P Weller, Robert M Tighe, and Timothy S Blackwell. Identification of myeloid cell subsets in murine lungs using flow cytometry. *American Journal of Respiratory Cell and Molecular Biology*, 49(2):180–189, aug 2013.

[85] Deepak Adhikari, Wenjing Zheng, Yan Shen, Nagaraju Gorre, Yao Ning, Guillaume Halet, Philipp Kaldis, and Kui Liu. Cdk1, but not cdk2, is the sole cdk that is essential and sufficient to drive resumption of meiosis in mouse oocytes. *Human Molecular Genetics*, 21(11):2476–2484, jun 2012.

[86] C Zheng, Q Yang, J Cao, N Xie, K Liu, P Shou, F Qian, Y Wang, and Y Shi. Local proliferation initiates macrophage accumulation in adipose tissue during obesity. *Cell death & disease*, 7:e2167, mar 2016.

[87] Clinton S Robbins, Ingo Hilgendorf, Georg F Weber, Igor Theurl, Yoshiko Iwamoto, Jose-Luiz Figueiredo, Rostic Gorbatov, Galina K Sukhova, Louisa M S Gerhardt, David Smyth, Caleb C J Zavitz, Eric A Shikatani, Michael Parsons, Nico van Rooijen, Herbert Y Lin, Mansoor Husain, Peter Libby, Matthias Nahrendorf, Ralph Weissleder, and Filip K Swirski. Local proliferation dominates lesional macrophage accumulation in atherosclerosis. *Nature Medicine*, 19(9):1166–1172, sep 2013.

[88] Diego Gómez-Nicola, Nina L Fransen, Stefano Suzzi, and V Hugh Perry. Regulation of microglial proliferation during chronic neurodegeneration. *The Journal of Neuroscience*, 33(6):2481–2493, feb 2013.

[89] Chayanon Ngambenjawong, Heather H Gustafson, and Suzie H Pun. Progress in tumor-associated macrophage (TAM)-targeted therapeutics. *Advanced Drug Delivery Reviews*, 114:206–221, may 2017.

[90] Ryo Yamasaki, Haiyan Lu, Oleg Butovsky, Nobuhiko Ohno, Anna M Rietsch, Ron Cialic, Pauline M Wu, Camille E Doykan, Jessica Lin, Anne C Cotleur, Grahame Kidd, Musab M Zorlu, Nathan Sun, Weiwei Hu, LiPing Liu, Jar-Chi Lee, Sarah E Taylor, Lindsey Uehlein, Debra Dixon, Jinyu Gu, Crina M Floruta, Min Zhu, Israel F Charo, Howard L Weiner, and Richard M Ransohoff. Differential roles of microglia and monocytes in the inflamed central nervous system. *The Journal of Experimental Medicine*, 211(8):1533–1549, jul 2014.

Abstract

Macrophage proliferation plays an essential role in the maintenance of tissue homeostasis, during an infection, and for the recovery after an injury, especially in tissues, where monocytic influx is inhibited, e.g. the brain. The cyclin-dependent kinase 1 (Cdk1) was the first kinase identified and is the 'master regulator' of the cell cycle. However, the role of Cdk1 in macrophages is unknown. Therefore, we generated a mouse-model with a Cdk1 deletion specific in myeloid cells, to determine the effect of Cdk1 on macrophage proliferation. Bone marrow-derived macrophages of Cdk1$^{fl/fl}$ $LysM^{cre/cre}$ mice were reduced and showed an impaired G2/M transition. Additionally, alveolar macrophages were also reduced *in vivo*. Large peritoneal macrophages were also reduced, but small periftoneal macrophages increased. Therefore, Cdk1 is important for the entry into mitosis during macrophage proliferation. In future, Cdk1 might me a promising target for pathologies, were macrophages proliferation either enhances or diminishes disease progression.

Zusammenfassung

Die Proliferation von Makrophagen spielt eine wichtige Rolle in der Aufrechterhaltung der Homeostase von Geweben, während Infektionen und in der Erholung nach Verletzungen, speziell in Geweben, wo keine Monocyten-Einströmung möglich ist, z.B.: im Gehirn. Die Cyclin-abhängige Kinase 1 (Cdk1) war die erste identifizierte Kinase und wird auch ' Hauptregulator' des Zellzykluses genannt. In einem Mausmodell mit einer Deletion von Cdk1 speziell in myeloiden Zellen wollten wir die Rolle von Cdk1 in Makrophage und den Effekt auf Makrophagen Proliferation untersuchen. Die Knochenmarksmakrophagen von $\text{Cdk1}^{fl/fl}$ $LysM^{cre/cre}$ Mäusen waren reduziert und zeigten einen gehinderten Übergang von der G2-Phase zu Mitose. Zusätzlich waren alveolare Makrophagen *in vivo* ebenfalls reduziert und Peritonealmakrophagen zeigten eine Zusammensetzung aus LPM und SPM vergleichbar mit der Zusammensetzung während einer Infektion. Diese Resultate weisen darauf hin, dass Cdk1 wichtig für den Eintritt in Mitose und die Proliferation von Makrophagen ist. In der Zukunft könnte Cdk1 ein vielversprechendes Ziel für Krankheiten sein, bei denen Makrophagen den Krankheitsverlauf entweder verschlechtern oder verbessern.